Applicability of dilution discharge measurements during flood wave conditions

Dec. 1987

R.M. Noppeney

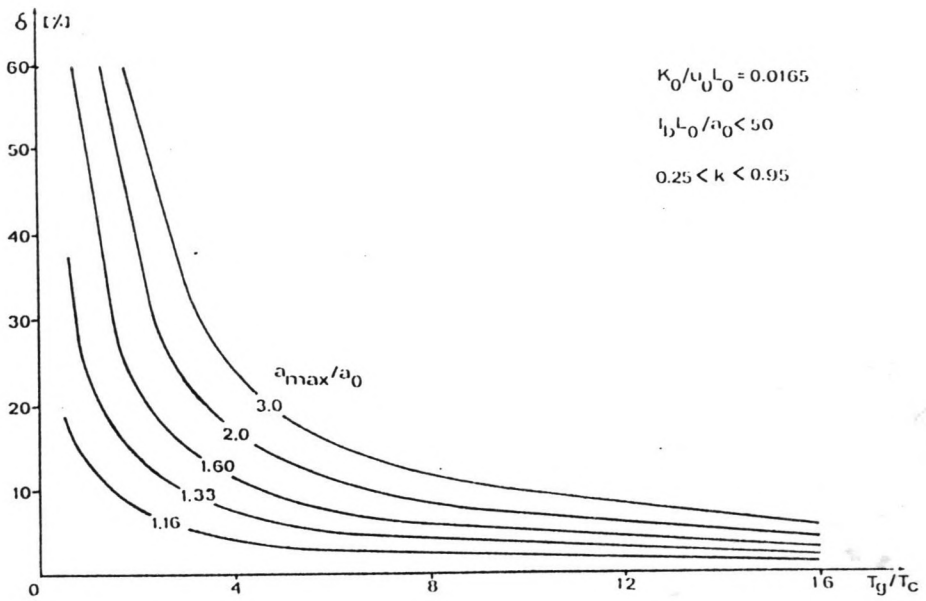

TU Delft
Delft University of Technology

Faculty of Civil Engineering
Hydraulic Engineering Group

APPLICABILITY OF DILUTION DISCHARGE MEASUREMENTS DURING FLOOD WAVE CONDITIONS

Report nr.

Rene Noppeney

M.Sc. Thesis

Dec. 1987

Thesis Supervisors:

Prof. M. de Vries

C. Kranenburg Ph.D.

A. van Mazijk M.Sc.

UNIVERSITY OF TECHNOLOGY DELFT

FACULTY OF CIVIL ENGINEERING

HYDRAULIC ENGINEERING GROUP

CONTENTS

PREFACE

This study is my M.Sc. thesis at the Department of Civil Engineering, Delft University of Technology.
I hereby wish to thank Prof. M. de Vries, C. Kranenburg Ph.D. and A. van Mazijk M.Sc. for their support and valuable suggestions throughout the past year.

René Noppeney

Dec. 1987

ABSTRACT

A severe restriction to dilution discharge measurements is that they are to be applied to steady flow conditions only.

Using a computational model, dilution discharge measurements by constant-rate injection are simulated during unsteady flow conditions caused by Gaussian flood waves propagating down a rectangular uniform channel.

The computational results are evaluated in order to provide a means of predicting a discharge measurement's accuracy.

The main source causing discrepancies between the actual and measured discharges is the difference in propagation velocities of the tracer cloud and the flood wave.

Correction procedures are recommended, since maximum inaccuracies can easily be larger by an order of magnitude than inaccuracies during steady-state conditions.

CHAPTER I INTRODUCTION

Measurements in open channel flow are conducted throughout the world and their aim is obvious: it is hard to think of a river engineering problem that might be solved without some data on river characteristics that can help shape the knowledge of a river's behaviour. Among river measurements, the measurement of discharges takes an important place, e.g. to establish a river's stage-discharge relationship.
There are several methods to measure discharges in open channel flow. Mention can be made of e.g. velocity-area methods, moving boat methods, slope-area methods or the use of discharge measurement structures such as weirs and flumes.
Dilution methods of measuring discharge have been known since at least 1863 (Kilpatrick and Cobb (1985)).
The principle of the method is simple. After injection and sufficient mixing of a tracer in a flow, the resulting concentration together with the known amount of released material determine the discharge.
To this end, both tracer and flow must fulfil several requirements.
The tracer must be soluble in water, not attaching to suspended sediments. The concentration resulting from injection must be measurable, without causing density currents. Until recently, chemical salts were generally used as tracers. Application of radio-active tracers is limited due to handling problems. Nowadays, stable fluorescent dyes, preferably Rhodamine WT (e.g. Wilson (1984)), together with fluorometers are used. Fluorometers measure the luminiscence of the fluorescent dye when it is subjected to a light source of a given wave length. The higher the concentration, the more emitted light is detected.
The requirement of sufficient mixing limits the use of dilution methods, from a practical point of view, to small streams. Over the river reach needed for sufficient mixing, the measurement's results are not to be disturbed by any unknown discharge contributions, e.g. from tributaries.
Under these conditions, the dilution method is particularly suitable when and where current meter measurements are impractical. This may be the case for small streams with excessive turbulence or debris, where the flow is inaccessible to man and/or measuring device, or where the cross-sectional area cannot be accurately measured.
A severe restriction is, that in view of a more or less sound theoretical background, dilution methods are restricted to steady flow conditions.
In this study the applicability of dilution discharge measurements during unsteady flow conditions caused by flood waves is investigated.
Problem and scope of this study are defined in Chapter II.
A mathematical model to determine the nature of the mixing processes involved is given in Chapter III.
Chapters IV and V treat analytical and numerical approaches to this model.
In Chapter VI the computational and analytical results are evaluated.
Conclusions and recommendations are presented in Chapter VII.

CHAPTER II PROBLEM

2.1 Introduction

Under steady flow conditions, both the constant rate and the slug injection technique can be used for injection. The distinction between the two methods lies in the time during which injection takes place.
Using the slug injection technique, a tracer amount m is, preferably instantaneously, injected. The discharge can be determined using the relationship (e.g. de Vries (1986)[1]):

$$m = Q \int_0^\infty (\phi(L,t) - \phi_i(L,t))dt$$

in which: m = released tracer amount
Q = discharge
ϕ = concentration
ϕ_i = initial (or 'background') concentration
L = mixing length (fig.1)
t = time

With the constant rate technique, a constant amount per unit time of tracer material is, preferably continuously, injected in the flow. In practice, the time during which injection has to take place is determined by reaching an equilibrium state: when, at the place of measurement, the concentration does not increase anymore (fig. 2), the discharge is determined by (e.g. de Vries (1986)[1]):

$$\phi(L) = \frac{M}{Q(L)} + \phi_i \qquad (1)$$

in which: M = released constant amount per unit time of tracer material

Since the flow is supposed to be steady and an equilibrium state is reached, time is, for constant initial concentration, of no influence in this relationship.
Both methods clearly show that for a good performance, the initial concentration should preferably be negligible with respect to the concentration resulting from injection.
If careful field and laboratory techniques are used, the relative error in the discharge determination is on the order of 1% (de Vries (1986)[1]).

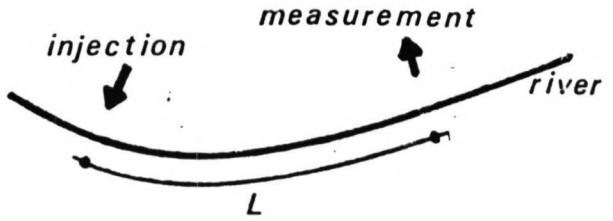

Fig 1 mixing length L

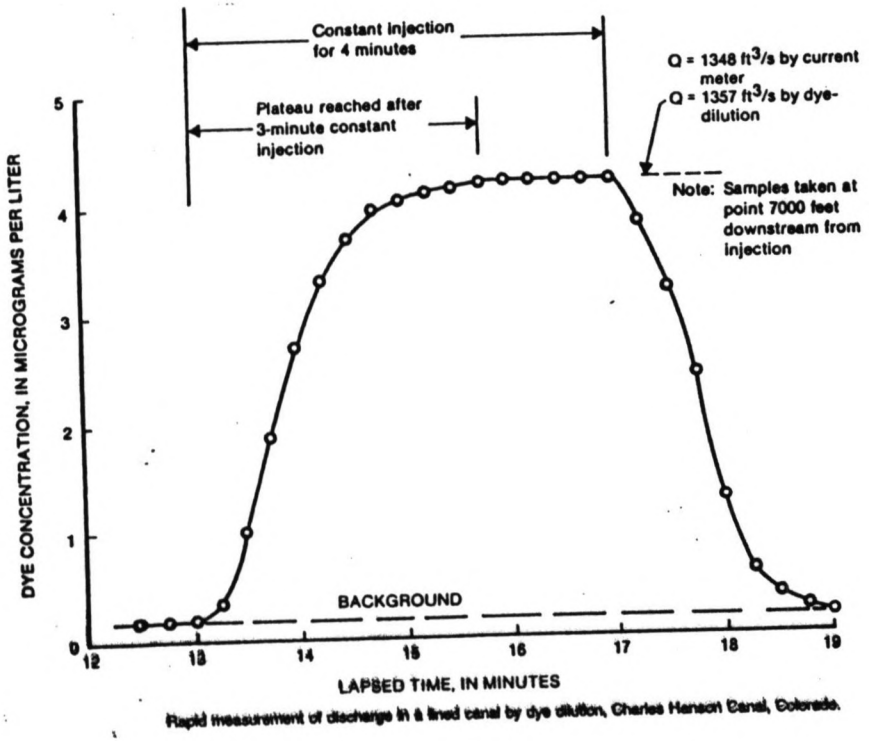

Kilpatrick and Cobb 1985

Fig 2 equilibrium development

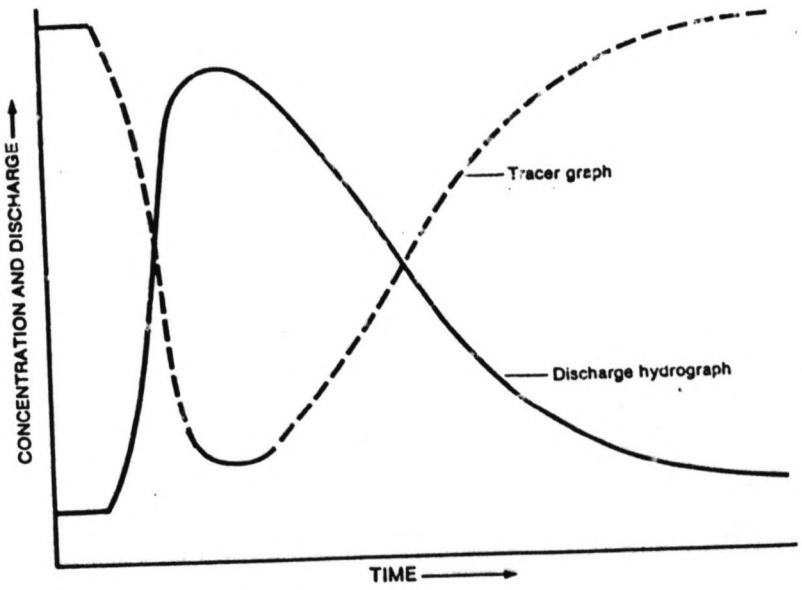

Fig 3 $\phi \equiv Q^{-1}$

2.2 Definition

Although a theoretical analysis of a continuous constant rate injection into unsteady open channel flow has not yet been accomplished, the nature of this discharge measurement method seems useful for measuring unsteady discharge conditions such as storm water run off events on small streams (Kilpatrick and Cobb (1985)).
In other words, straightforward extension of the constant rate method would mean extension of eq. (1), neglecting the initial concentration, to (fig. 3):

$$\phi(L,t) = \frac{M}{Q(L,t)} \qquad (2)$$

It is the applicability of this eq. (2) that is investigated in this study.

2.3 Aim, Approach and Restrictions

Since eq. (2), though practical, is theoretically incorrect, the aim of this study is to determine a relation to qualify and quantify the errors made when using eq. (2) for discharge measurements during unsteady flow.
To this end, the influence of flood waves on concentrations resulting from a constant rate injection into a channel of rectangular, uniform cross-section is studied. Other common environmental unsteady types of flow, such as tidal flows, have not been taken into consideration.
The approach has been merely analytical and numerical. Field- and/or laboratory experiments have not been performed.

CHAPTER III MATHEMATICAL MODEL

3.1 Introduction

Since it is widely accepted that man's conception of his world is three-dimensional, and there is, for the time being, no reasonable alternative to this assumption, it may be assumed that all environmental processes occur in three dimensions. Therefore, a mathematical model describing physical environmental processes should be formulated in these three dimensions.
Moreover, since man and nature itself provide ever changing boundary conditions to environmental processes, such a model should also incorporate time: striving for a new equilibrium state requires time. This only seems to complicate things, and it often does.
Sometimes, however, depending on the nature of the physical environmental processes involved, the concept of time can also be used to simplify things.
Imagine the release of a soluble substance in a river. A river has the pleasant property that one spacial dimension clearly dominates the other two: its width and depth are much smaller than its length. Therefore the solute will mix relatively quickly in vertical and transverse directions. After the solute has been mixed homogeneously over the river's cross-section, the mixing process can be described using only one spatial dimension. The mathematical model to arrive at in Section 2 uses this feature and approximates the mixing process in the longitudinal direction only.
Not just any model will do. The aim in modeling nature is satisfying accuracy. Despite the most sophisticated attempts, the model itself often provides a major source of inaccuracy. Nature is complex and lack of knowledge of its processes calls for simplifications. Generally speaking, these simplifications do not tend to increase accuracy.
Degenerating an environmental process to one dimension adds at least two (related) problems to the existing ones. Some parameters, maybe already vaguely known, should be chosen such, that the approximation is still satisfying compared to a three-dimensional model. Secondly, a one-dimensional model cannot describe essentially three-dimensional processes. So the model cannot describe the initial period, before mixing over the river's cross-section is completed. Section 2 of this Chapter illustrates this in describing dispersion processes, a dispersion coefficient and a mixing length.
In Section 3, the second one-dimensional model, that for flood waves, is given.
Section 4 describes the approach used to dispersion during flood waves.

3.2 Dispersion

3.2.1 Introduction

In arriving at an equation that describes the dispersion process of a released substance in open channel flow, several assumptions about the released substance and the receiving water have to be made.
The substance is assumed to move with the water. It does not have its own specific mode of transportation. Dissolved matter, heat and very fine particles have this property some time after their release when the effects of initial momentum and buoyancy due to their release have decayed.
The release is supposed to cause no density currents. Generally speaking, this means that the substance is low concentrated and causes no density differences large enough to influence the flow field after initial dilution.
Under these assumptions, corresponding to the tracer requirements, several modes of transportation occur. These may be subdivided into two: convection and dispersion. The distinction between the two depends on the process involved in relationship to the scale of the whole system.
Large scale flow carries a cloud of released substance as a whole. This transportation mode is denoted by convection.
Water motion on a scale small compared to the size of the cloud of material results in a type of mixing denoted by the term dispersion.
A cloud of material which is small relative to the scale of turbulent eddies will be subject only to molecular diffusion.
As the cloud grows larger, turbulent diffusion is included in the dispersion process.
When mixing over the depth of the channel has been accomplished, dispersion due to vertical non-uniformity of the flow velocity profile becomes important.
Some time later, the cloud will occupy the whole cross-section and dispersion by transverse non-uniformity is important.

3.2.2 Molecular Diffusion

Usually, molecular diffusion can be neglected in large scale dispersion processes. Since, however, dispersion as a whole may be described analogous to molecular diffusion, a short analysis is given here.
Consider a control volume in a laminar flow field (fig. 1). Conservation of mass states that the time rate of change of mass equals the difference in mass flux. Flux is the mass crossing a unit area per unit time in a given direction.

For a conservative substance, this yields in one dimension:

$$\frac{\delta \phi}{\delta t} + \frac{\delta F_x}{\delta x} = 0$$

in which: F_x = flux in x-direction

The flux consists of a convective and a diffusive part. The convective flux is the rate at which fluid volume passes through a unit area, multiplied by the concentration of mass in that volume:

$$F_{x,conv} = u\phi$$

in which: u = flow velocity in x-direction

The diffusive flux can be described by Fick's law. This law assumes that the diffusive flux of a solute mass is proportional to the gradient of the solute concentration in that direction:

$$F_{x,diff} = -D \frac{\delta \phi}{\delta x}$$

in which: D = molecular diffusion coefficient.

The negative sign indicates transport to take place from high to low concentration areas.
Assuming the convective and diffusive flux to be additive yields:

$$F_x = u\phi - D \frac{\delta \phi}{\delta x}$$

and so it follows, since D is a constant:

$$\frac{\delta \phi}{\delta t} + \frac{\delta}{\delta x}(u\phi) - D \frac{\delta^2 \phi}{\delta x^2} = 0$$

Extension to three dimensions is more or less straightforward and yields:

$$\frac{\delta \phi}{\delta t} + \frac{\delta}{\delta x}(u\phi) + \frac{\delta}{\delta y}(v\phi) + \frac{\delta}{\delta z}(w\phi) - D\left(\frac{\delta^2 \phi}{\delta x^2} + \frac{\delta^2 \phi}{\delta y^2} + \frac{\delta^2 \phi}{\delta z^2}\right) = 0 \qquad (3)$$

in which: v = flow velocity in y-direction
w = flow velocity in z-direction

Fig 1

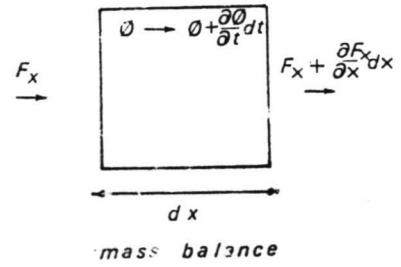

mass balance

Fig. 2 Averaging of turbulent fluctuations. Note: this is a schematic representation; in reality the time-scale of the mean velocity $\bar{u}$ will be much larger relative to the time-scale of turbulence

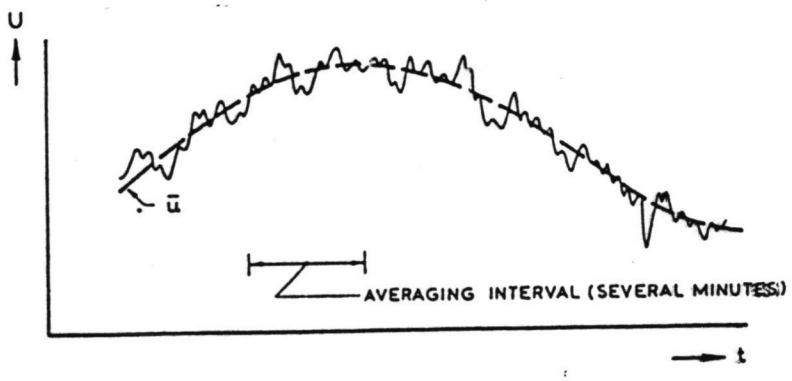

Jansen 1979

3.2.3 Turbulent Diffusion

The diffusion process in turbulent flow is considerably more complicated. Mass introduced in turbulent flow will spread much faster than in laminar flow. Velocities and pressures in the flow field are unsteady and posess an appreciable random component. It is customary to apply a time averaging procedure in order to distinguish between the mean flow and these turbulent fluctuations. This procedure assumes that the instantaneous velocities (and concentrations) can be seen as the sum of a time averaged and a fluctuating component:

$$\phi = \bar{\phi} + \phi'$$

$$u = \bar{u} + u'$$

$$v = \bar{v} + v'$$

$$w = \bar{w} + w'$$

in which: $\bar{\phi} = \frac{1}{T} \int_{t}^{t+T} \phi dt$

and so on.

The averaging period T is supposed to be sufficiently long to permit convergence of the averages of the fluctuating components to zero, yet not so long as to significantly damp the variation of the time-averages with t (fig. 2).
Substitution in eq.(3) and neglecting molecular diffusion yields:

$$\frac{\delta}{\delta t}(\bar{\phi} + \phi') + \frac{\delta}{\delta x}(\bar{u} + u')(\bar{\phi} + \phi') + \frac{\delta}{\delta y}(\bar{v} + v')(\bar{\phi} + \phi') +$$

$$+ \frac{\delta}{\delta z}(\bar{w} + w')(\bar{\phi} + \phi') = 0$$

Averaging this equation over a time T as indicated above yields (e.g. de Vries (1984)[2]):

$$\frac{\delta \phi}{\delta t} + \frac{\delta}{\delta x}\overline{u\phi} + \frac{\delta}{\delta y}\overline{v\phi} + \frac{\delta}{\delta z}\overline{w\phi} + \frac{\delta}{\delta x}\overline{u'\phi'} + \frac{\delta}{\delta y}\overline{v'\phi'} + \frac{\delta}{\delta z}\overline{w'\phi'} = 0$$

In the last three terms, the time averages of a product of fluctuating velocity and concentration represent mixing through turbulent diffusion. The obvious approach is to express these terms as time-mean quantities.

This may be done by Reynold's analogy, which concept leads to a turbulent diffusion tensor T_{ij} that can be written, using the Einstein summation convention, as (e.g. Sayre (1975)):

$$T_{ij}\,\frac{\delta \phi}{\delta x_j} = -\overline{\phi' u'_j} \qquad \text{for } i,j = 1,2,3$$

in which: $x = (x_1, x_2, x_3)$ or (x,y,z) vector notation

$u = (u_1, u_2, u_3)$ or (u,v,w) vector notation

Although this local gradient type transport description is not exact, since with the larger length scales of turbulence, the gradients will vary over these length scales, for computations the assumption of a gradient type transport is believed to be sound enough (e.g. Booij (1986)).
Inserting the diffusion tensor and omitting the time-mean overbars, which are no longer needed, gives:

$$\frac{\delta \phi}{\delta t} + \frac{\delta}{\delta x}(u\phi) + \frac{\delta}{\delta x}(v\phi) + \frac{\delta}{\delta x}(w\phi) +$$

$$- \frac{\delta}{\delta x}\left(T_{xx}\frac{\delta \phi}{\delta x}\right) - \frac{\delta}{\delta y}\left(T_{yy}\frac{\delta \phi}{\delta y}\right) - \frac{\delta}{\delta z}\left(T_{zz}\frac{\delta \phi}{\delta z}\right) +$$

$$- \frac{\delta}{\delta x}\left(T_{xy}\frac{\delta \phi}{\delta y}\right) - \frac{\delta}{\delta y}\left(T_{yz}\frac{\delta \phi}{\delta z}\right) - \frac{\delta}{\delta z}\left(T_{zx}\frac{\delta \phi}{\delta x}\right) +$$

$$- \frac{\delta}{\delta x}\left(T_{xz}\frac{\delta \phi}{\delta z}\right) - \frac{\delta}{\delta y}\left(T_{yx}\frac{\delta \phi}{\delta x}\right) - \frac{\delta}{\delta z}\left(T_{zy}\frac{\delta \phi}{\delta y}\right) = 0$$

It is customary (e.g. Sayre (1975)) to assume the coordinate axes to coincide with the principal axes of the diffusion tensor, leaving:

$$\frac{\delta \phi}{\delta t} + \frac{\delta}{\delta x}(u\phi) + \frac{\delta}{\delta x}(v\phi) + \frac{\delta}{\delta x}(w\phi) +$$

$$- \frac{\delta}{\delta x}\left(T_{xx}\frac{\delta \phi}{\delta x}\right) - \frac{\delta}{\delta y}\left(T_{yy}\frac{\delta \phi}{\delta y}\right) - \frac{\delta}{\delta z}\left(T_{zz}\frac{\delta \phi}{\delta z}\right) \approx 0 \qquad (4)$$

Fischer (1979) justifies this procedure by stating that in a wide channel it is reasonable to expect coefficients for vertical, transverse and longitudinal mixing, because the boundaries at surface and bottom create a turbulence that will not be isotropic. Thus it can be assumed that there are no other tensor coefficients since there is no preferred diagonal direction of motion as long as the axes are parallel and perpendicular to the bottom.
The main obstacles to progress from here have been the lack of a reliable theory that relates the spacial variation of T_{xx}, T_{yy} and T_{zz} to flow and boundary conditions. Experimental studies in straight rectangular channels indicate that (e.g. Fischer (1979)):

$$T_{zz} \approx 0.06 \cdot a u_*$$

in which: a = depth of flow
u_* = bottom friction velocity
T_{zz} = vertical diffusivity

$$T_{yy} \approx 0.15 \cdot a u_*$$

in which: T_{yy} = transverse diffusivity

The longitudinal turbulent mixing coefficient T_{xx} is believed to be of the same order of magnitude as the transverse mixing coefficient T_{yy}:

$$T_{xx} \approx 0.15 \cdot a u_*$$

in which: T_{xx} = longitudinal diffusivity

Rates of turbulent longitudinal mixing have not been measured actually. This is due to difficulties in separating longitudinal mixing caused by turbulence and longitudinal mixing caused by shear flow.

3.2.4 Shear Flow Dispersion

Common to river flows is that mixing in flow direction is caused primarily by the velocity profile in the cross-section (fig. 3). If, after release, a tracer cloud has grown large enough to occupy the river's cross-section, it makes sense, in view of a one-dimensional description, to integrate eq. (4) over the cross-section A. This yields, with double overbars denoting cross-sectional means (e.g. Berkhoff (1973)):

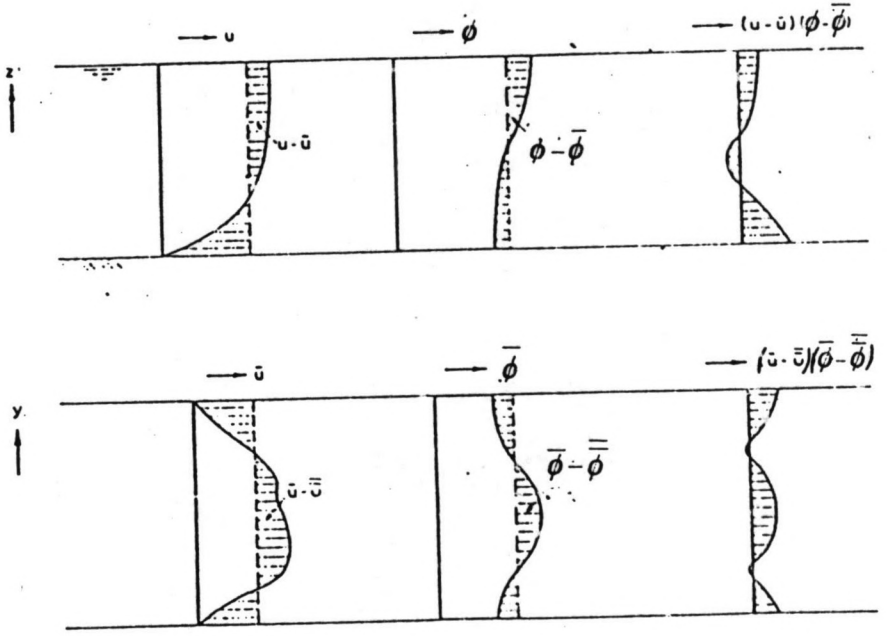

Fig. 3 Illustration of dispersion by vertical non-uniformity (top) and by lateral non-uniformity (bottom)

Jansen 1979

$$\frac{\delta}{\delta t}(A\bar{\phi}) + \frac{\delta}{\delta x}(Au\bar{\phi}) - \frac{\delta}{\delta x}(AT_{xx}\frac{\delta\bar{\phi}}{\delta x}) = 0$$

in which: A = river's cross-section

In arriving at this equation it is assumed that no diffusive flux passes lateral boundaries or water surface.
Splitting up the velocity and concentration in the following way:

$$\phi(x,y,z,t) = \bar{\phi}(x,t) + \phi''(x,y,z,t)$$

$$u(x,y,z,t) = \bar{u}(x,t) + u''(x,y,z,t)$$

in which: $$\bar{\phi}(x,t) = \frac{1}{A}\iint_A \phi dydz$$

and so on,

and inserting these yields:

$$\frac{\delta}{\delta t}(A\bar{\phi}) + \frac{\delta}{\delta x}(A\bar{u}\cdot\bar{\phi}) + \frac{\delta}{\delta x}(\overline{Au''\phi''}) - \frac{\delta}{\delta x}(AT_{xx}\frac{\delta\bar{\phi}}{\delta x}) = 0$$

An order of magnitude analysis indicates that dispersion by cross-sectional non-uniformity exceeds turbulent diffusion by far (e.g. Jansen (1979)). So:

$$\frac{\delta}{\delta t}(A\bar{\phi}) + \frac{\delta}{\delta x}(A\bar{u}\cdot\bar{\phi}) + \frac{\delta}{\delta x}(\overline{Au''\phi''}) = 0$$

The obvious approach, again, is to express the last term in terms of cross-sectional means. A general procedure, however, is not available. Widely used in river engineering is the Taylor method. Sir G.I. Taylor assumed (in 1953) that the cross-sectional concentration profile $\phi''(y,z)$ is established by a balance between longitudinal convective transport and cross-sectional diffusive transport, yielding a 'Fickian approach' type of relationship:

$$\overline{Au''\phi''} = -AK\frac{\delta\bar{\phi}}{\delta x}$$

in which: $$K = -\frac{1}{A}\iint_A u''f(y,z)dydz$$ = dispersion coefficient

The function $f(y,z)$ is defined by: $\phi'' = f(y,z)\frac{\delta\bar{\phi}}{\delta x}$

Inserting yields the dispersion equation:

$$\frac{\delta}{\delta t}(A\phi) + \frac{\delta}{\delta x}(Au\cdot\phi) - \frac{\delta}{\delta x}\left(AK\frac{\delta\phi}{\delta x}\right) = 0 \qquad (5)$$

Fischer (1967) gave a quantitative estimate of the dispersion coefficient in natural streams, by assuming a balance between longitudinal convection and transverse diffusion, neglecting the vertical profile entirely (fig. 4). The function f(y,z) then has the form:

$$f(y) = \int_0^y \frac{1}{aT_{yy}} \int_0^y u''a\,dy\,dy$$

and K can be written as:

$$K = -\frac{1}{A}\int_0^B u''a \int_0^y \frac{1}{aT_{yy}} \int_0^y u''a\,dy\,dy\,dy$$

in which: B = river's width

under the assumption that u" does not vary with z (or x). Laboratory and field experiments yield from this expression the more workable form (e.g. Fischer (1979)):

$$K = 0.011\cdot\frac{u^2B^2}{au_*} \qquad (6)$$

in which a value $T_{yy} = 0.6\cdot au_*$ is used.

In most cases, eq. (6) has been found to agree within a factor 4, which is, in fact, quite accurate bearing in mind all the possible irregularities contributing to dispersion that can be found in rivers. Moreover, eq. (6) has the advantage of predicting dispersion from usually available parameters.
Using a value:

$$T_{yy} = kau_* \qquad (7)$$

in which: k = coefficient of proportionality

eq. (6) can be written as:

$$K = 0.0066\cdot\frac{u^2B^2}{T_{yy}} \qquad (8)$$

The value of k in natural streams is given by (Fischer (1979)):

$k \approx 0.6 \pm 0.3$

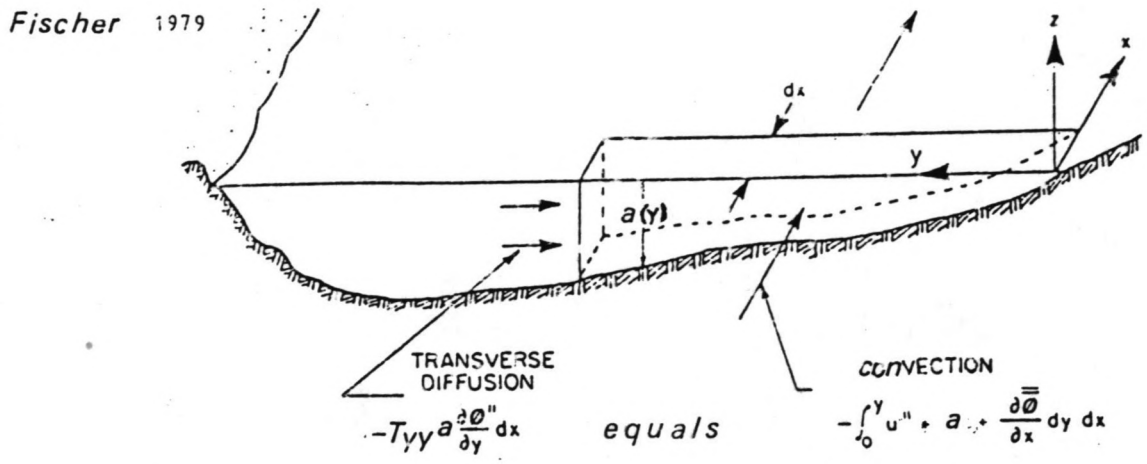

Figure 4 . An illustration of the balance: convection and diffusion

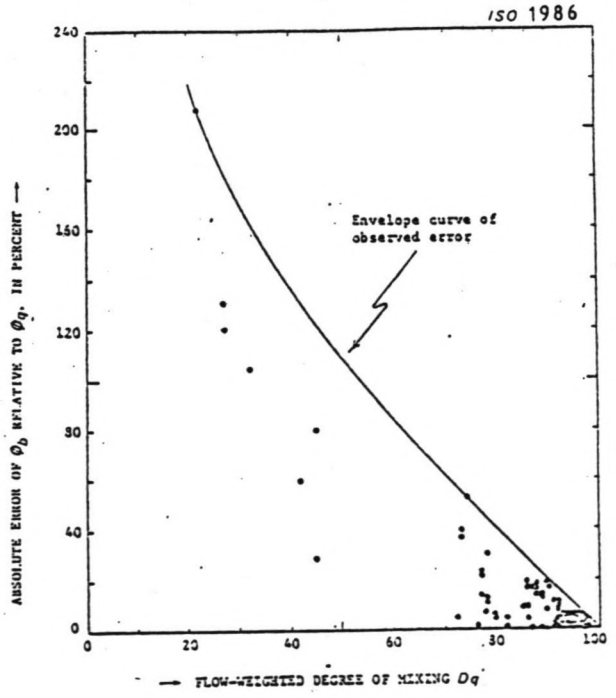

Figure 5 Envelope curve of observed error in the width-weighted computation of mean concentration.

3.2.5 Mixing Lengths

3.2.5.1 introduction

The essence of the Taylor method is, that the assumed balance between longitudinal convection and cross-sectional diffusion is reached under some circumstances. Essentially this boils down to the requirements that (Fischer (1979)):

$\bar{\phi}$ is varying slowly along the channel,

$\delta\bar{\phi}/\delta x$ is essentially constant over a long period of time,

ϕ'' has become small compared to $\bar{\phi}$.

The last requirement is reached when cross-sectional diffusion has evened out cross-sectional gradients.
The first two requirements concern the longitudinal direction. For the 'Fickian approach' to dispersion to be valid, they are fulfilled when the longitudinal concentration profile, originating from an instantaneous release, behaves like a Gaussian distribution.

3.2.5.2 cross-sectional mixing

A variety of empirical as well as (semi) theoretical formulas have been developed for estimating cross-sectional mixing lenghts in open channel flow. Apart from properties of the released substance, this mixing length is a function of the degree of mixing, place and way of release and channel and flow properties. Generally all formulas are developed for a condition that is supposed to represent complete cross-sectional mixing. This, however, would require an infinite mixing length which is not very practical.
The actual degree of mixing can best (ISO (1986)) be estimated using the Cobb-Bailey formula:

$$D_Q = \left[1 - \tfrac{1}{2} \sum_{j=1}^{n} \left|\frac{\phi_j - \phi_Q}{\phi_Q}\right| \left(\frac{q_j}{Q}\right)\right] * 100\%$$

in which: D_Q = flow weighted degree of mixing
ϕ_j = concentration in the j-th segment
$\phi_Q = \frac{1}{Q} \sum_{j=1}^{n} \phi_j q_j$
q_j = flow in segment j
n = number of segments in a cross-section

If no information is available on the variation of the discharge over the cross-section (as will be the case with most discharge measurements), an approximate procedure is to substitute a relative width in place of the relative discharge in the Cobb-Bailey formula. The error in determining mean concentrations using the width-weighted formula is given in fig. 5 as a function of the flow-weighted degree of mixing. This envelope curve is based on uniform and non-uniform cross-sections. Clearly, the more uniform the section, the smaller the error, which, however, cannot directly be concluded from fig. 5.
The (semi) theoretical approach to mixing lengths provides the most universal relationships, that are not site-specific and thus have the bigger transfer value.
For releases at the centre of flow and at river banks, the Fischer formula provides an easy in use and accurate estimate of the mixing length for a degree of mixing of 95% (e.g. van Mazijk (1984)). Essentially it is based on a characteristic time scale for mixing. From dimensional reasoning, it follows that such a time scale T_c must be proportional to the square of a characteristic length, divided by a characteristic diffusivity, both depending on channel and flow properties (Fischer (1979)). Setting a dimensionless time T_d, this can be written as:

$$T_d = \frac{D_c}{L^2_c} t = \frac{t}{T_c}$$

in which: T_d = dimensionless time
D_c = characteristic diffusivity
L_c = characteristic length
T_c = characteristic time

Having a turbulent flow down a channel of finite width, a characteristic length will have order of magnitude of the channel's width and a characteristic diffusivity can be seen as the transverse diffusivity T_{yy}. So:

$$T_c \approx \frac{B^2}{T_{yy}} \qquad (9)$$

From an approximate solution for mixing from a maintained line source in a steady uniform flow in two dimensions, Fischer found that, for a dimensionless distance $X_d > 0.1$ the concentration is within 5% of its mean value of the cross-section after a centre line release and for $X_d > 0.4$ this degree of mixing is reached after a side injection, in which:

$$X_d = \frac{x}{u_0 T_c}$$

This yields:

$$L_{o,95} = 0.4 \frac{u\,B^2}{T_{yy}} \quad \text{for a side release}$$

$$L_{o,95} = 0.1 \frac{u\,B^2}{T_{yy}} \quad \text{for a centre release}$$

in which: $L_{o,95}$ = cross-sectional mixing length for 95% mixing

3.2.5 3 longitudinal mixing

Apart from evening out cross-sectional differences it is necessary for the cross-sectional averaged concentration to decay towards a Gaussian distribution.
Numerical experiments in uniform channel flow have shown that the variance of a dispersing cloud grows linearly with distance downstream for $X_d > 0.2$ (Fischer (1979)). Linear growth of the variance σ^2 is a necessary condition for the diffusion to apply, but not a sufficient one. Only after $X_d > 0.4$, the skewed dispersing cloud starts decaying towards a Gaussian distribution and for $X_d > 1$ the longitudinal distribution is expected to become approximately Gaussian (fig. 6)).
A numerical analysis by Sayre (1975) indicates the initial period during which Taylor's method does not apply, determined by $T_d > 0.5$ (fig. 7).
As always, real streams complicate things. Sometimes streams are so irregular, that Taylor's method does not apply throughout the whole flow field. Nevertheless, the majority of streams are uniform enough for an approximate analysis. Incorporating moderate irregularities, Fischer (1979) uses a value of $X_d = 0.4$ as a limit to the initial zone. So:

$$L_i = 0.4 \frac{uB^2}{T_{yy}} \qquad (10)$$

in which: L_i = length of initial zone

Fischer 1979

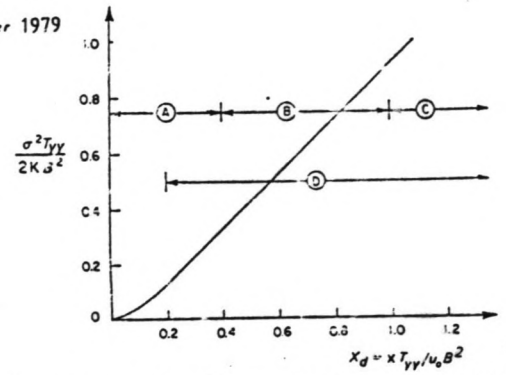

Figure 6 Stages in the evolution of a concentration distribution from a slug injection and expected growth of the longitudinal variance as given by numerical experiments in uniform channels. In real channels sidewall irregularities will increase the required values of X_d

Ⓐ Generation of a skewed distribution. Ⓑ Decay of the skewed distribution.
Ⓒ Approach to a Gaussian distribution. Ⓓ Zone of linear growth of the variance.

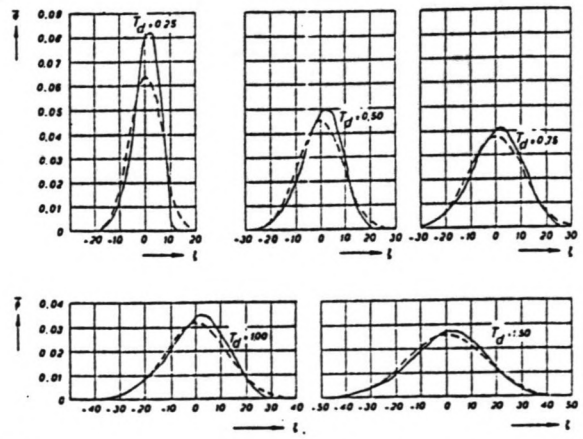

FIG. 7

—— ESTIMATED FROM PEARSON TYPE III DISTRIBUTION (THE ARIS METHOD)
– – – GAUSSIAN DISTRIBUTION
$t = (x - G1)/\sigma$

Sayre 1975

3.3 Flood Waves

3.3.1 Introduction

This section gives a somewhat informal derivation of the flood wave equations. A much more sophisticated approach can be found in e.g. Verspuy and De Vries (1981).
The last three subsections discuss simplifications of the long wave equations, that, under certain circumstances can be applied to the special case of flood waves.

3.3.2 Equation of Continuity

Consider a control volume in an open channel flow with cross-section A (fig. 8). Conservation of mass states that the change of mass equals its net inflow. For constant density, this yields, with $\delta/\delta s \approx \delta/\delta x$, since is is small:

$$(A+\frac{\delta A}{\delta x}dt)dx - Adx = Audt - (Au + \frac{\delta}{\delta x}(Au)dx)dt$$

and so:

$$\frac{\delta A}{\delta t} + \frac{\delta}{\delta x}(Au) = 0$$

For constant width B and A=B·a this yields:

$$\frac{\delta a}{\delta t} + u\frac{\delta a}{\delta x} + a\frac{\delta u}{\delta x} = 0 \qquad (11)$$

3.3.3 Momentum Equation

Consider again the control volume (fig. 8). Newton's second law states that the change of momentum in time in a certain direction equals all forces working in that direction, which can be written as:

$$\frac{\delta}{\delta t}(\rho Bau)ds + \frac{\delta}{\delta s}(\rho Bauu)ds = \Sigma F_s$$

in which: ρ = density

The second term on the left hand side accounts for net flux of

fig 8

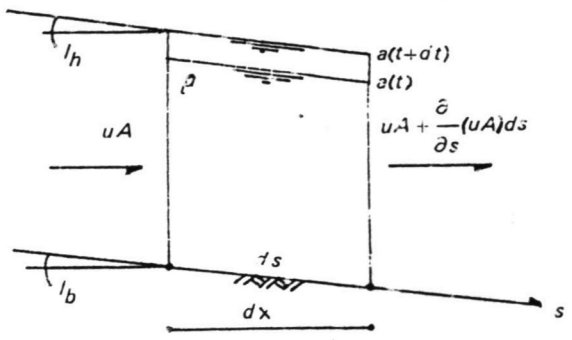

mass balance

fig 9

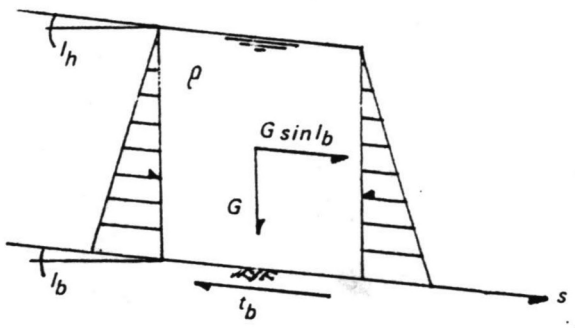

Forces

momentum.
It is now necessary to evaluate the forces F_s working on the control volume. For long waves, the pressure is hydrostatic. So on both sides of the volume, a hydrostatic pressure force is working. Other forces working are the flow directed component of the mass gravity force and the bottom friction τ_b. Neglecting other influences such as wind-driven forces or the Coriolis force, this yields (fig. 9), neglecting higher order terms:

$$\Sigma F_s = (-\rho g a \frac{\delta a}{\delta s} ds + \rho g a \cdot \sin(i_b) \cdot ds - \tau_b \cdot ds) B$$

in which: g = gravity force
τ_b = bottom friction

Inserting this in the momentum equation yields, after dividing by $\rho b ds$:

$$\frac{\delta}{\delta t}(au) + \frac{\delta}{\delta s}(au^2) + ga\frac{\delta a}{\delta s} - ga \cdot \sin(i_b) + \frac{\tau_b}{\rho} = 0$$

Since i_b is small, it follows $\frac{\delta}{\delta s} \approx \frac{\delta}{\delta x}$ and $\sin(i_b) \approx i_b$ and so, after differentiation:

$$u\left(\frac{\delta a}{\delta t} + u\frac{\delta a}{\delta x} + a\frac{\delta u}{\delta x}\right) + a\frac{\delta u}{\delta t} + au\frac{\delta u}{\delta x} + ga\frac{\delta a}{\delta x} - gai_b + \frac{\tau_b}{\rho} = 0$$

The first term vanishes applying the continuity eq. (11). Dividing by a then yields:

$$\frac{\delta u}{\delta t} + u\frac{\delta u}{\delta x} + g\frac{\delta a}{\delta x} - gi_b + \frac{\tau_b}{a\rho} = 0$$

The bottom friction term τ_b in steady uniform flow can be written as (e.g. Verspuy and de Vries (1981)):

$$\tau_b = \rho g \frac{u^2}{C^2}$$

in which: C = Chézy coefficient

If the flow is slightly unsteady, such as with flood waves, this relationship is still assumed to hold. So:

$$\frac{\delta u}{\delta t} + u\frac{\delta u}{\delta x} + g\frac{\delta a}{\delta x} - gi_b + g\frac{u^2}{C^2 a} = 0 \qquad (12)$$

3.3.4 Kinematic approach

In a first approximation, it could be assumed that fluctuations in the discharge are so slow that the first three terms in eq. 12 are small compared to the last two terms, leaving:

$$-gi_b + g\frac{u^2}{C^2 a} = 0$$

or:

$$u = C\sqrt{(ai_b)}$$

which is the Chézy equation.

Introducing the Chézy eq. in the continuity eq. yields:

$$\frac{\delta a}{\delta t} + \frac{3}{2} u \frac{\delta a}{\delta x} = 0$$

for constant slope and roughness.

This equation describes the propagation of a kinematic wave. The square friction relationship $\tau_b \equiv u^2$ yields a propagation velocity $c=1.5 \cdot u$.

3.3.5 Diffusion Analogy

Where damping of flood waves is important, the kinematic approach does not give a realistic picture. A more appropriate theory can then be obtained by retaining the water surface slope in the momentum equation. Eq. (12) thus degenerates into:

$$g\frac{\delta a}{\delta x} - gi_b + g\frac{u^2}{C^2 a} = 0$$

or:

$$u^2 = C^2 a i_b - C^2 a \frac{\delta a}{\delta x}$$

Differentiation with respect to x yields:

$$\frac{\delta u}{\delta x} = \frac{C^2 i_b}{2u}\frac{\delta a}{\delta x} - \frac{C^2}{2u}\left(\frac{\delta a}{\delta x}\right)^2 - \frac{C^2 a}{2u}\frac{\delta^2 a}{\delta x^2}$$

Inserting this in the continuity eq. (11) yields:

$$\frac{\delta a}{\delta t} + \frac{3}{2} u \frac{\delta a}{\delta x} - \frac{C^2 a^2}{2u} \cdot \frac{\delta^2 a}{\delta x^2} = 0$$

The third term now causes damping. The coefficient $C^2a^2/2u$ has dimensions L^2T^{-1} and is analogous to a diffusion coefficient.

3.3.6 Evaluation

When peak flows lasting only a few hours occur, even the diffusion analogy may not give a good description. Then there is no alternative to using the full dynamic eq. (12).
An attempt to quantify the differences between the three approaches is given by Grijsen and Vreugdenhil (1976). It is based on a linearization of the momentum equations.
In fig. 10a the velocities of propagation c of the three approaches are compared and in fig. 10b the damping lengths L_e, the lengths over which the wave height is reduced by a factor e^{-1}. The kinematic approach does not allow damping.
Both comparisons in these figures are given as functions of the Froude number Fr and a parameter E. For the unit width approach, they are:

$$Fr = \frac{u}{\sqrt{ga}} \qquad (13)$$

$$E = \left(\frac{g^3 T_0^2}{C^4 a}\right)^{\frac{1}{2}} \qquad (14)$$

in which T_0 is the 'period' of the flood wave.

As can be seen from fig. 10, the larger E, the more accurate the results for wave propagation compared to the dynamic situation. Wave damping, however, is systematic in error. Especially at large Froude numbers, a serious underestimate of the rate of damping can be found using the diffusion analogy.
This error may be reduced by applying a correction proposed by van de Nes and Hendrikse (1971). They state that, instead of evaluating the coefficients in the (linearized) equations at the steady flow situation prior to the wave passage, a choice of a mean value within the actual range of the variables gives the better reference situation.

fig 10 Comparison of diffusion analogy (solid lines) and kinematic wave approach (dashed lines) with complete theory.

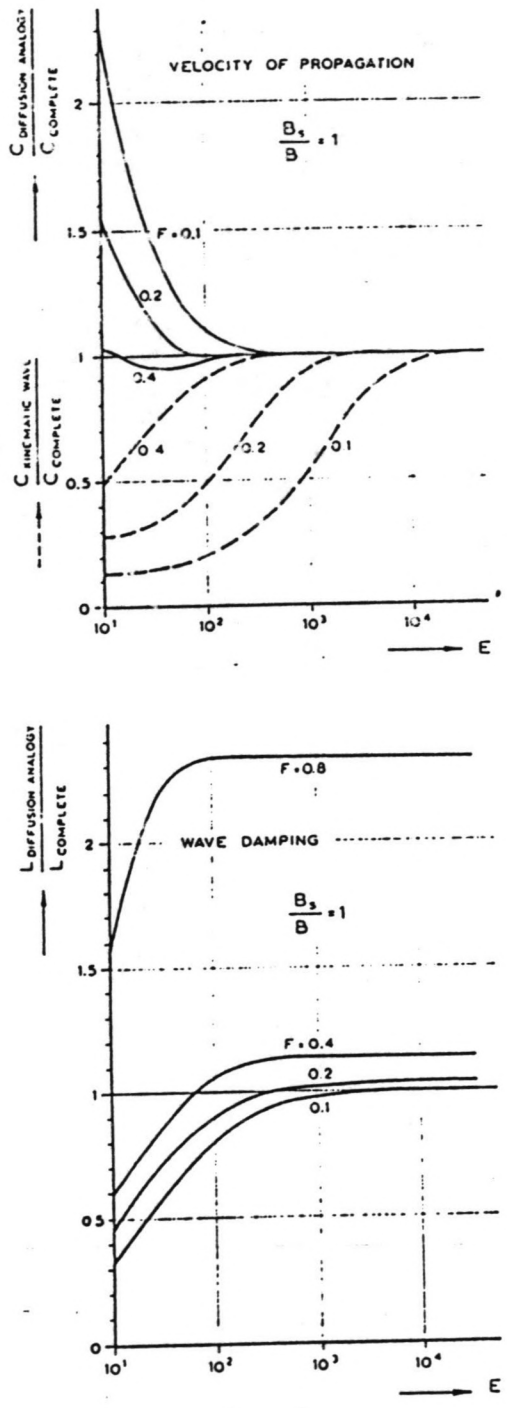

Jansen 1979

3.4 Dispersion during Flood Waves

The flow cases treated in the previous section are unsteady whereas the dispersion coefficient by Taylor's method essentially is derived for steady and uniform flow. Extension of Taylor's analysis to unsteady flow, has, in the case of purely oscillating flow been done by e.g. Holley,Harleman and Fischer (1970) and Chatwin (1975).
For both approaches it is possible to distinguish between two limiting cases, depending on the flow period of oscillation T_0 and the characteristic dispersion time T_c (Fischer (1979)).
Suppose $T_0 >> T_c$. In that case the concentration profile ϕ" will have sufficient time to adapt to the changing velocity profile. In other words, the time required for ϕ" to reach a concentration profile is short compared to the time during which ϕ" actually has that profile. So a dispersion coefficient of the same nature as in steady flow can be expected.
In the opposite limit, $T_0 << T_c$, the concentration profile gets not enough time to adjust to the changing velocity profile. In purely oscillating flow, ϕ" can be assumed to oscillate around the mean of the symmetric profiles, which is zero. So, in this limit, the dispersion coefficient tends to zero (fig. 11).
Intermediate behaviour of the dispersion coefficient may be given by:

$$\overline{K_{osc}} = K_0 \cdot f\left(\frac{T_0}{T_c}\right)$$

in which: $\overline{K_{osc}}$ = cycle averaged dispersion coefficient in an oscillating flow with velocity amplitude $\hat{u}$

K_0 = dispersion coefficient in steady flow with velocity $u0 = \hat{u}$

f = function of T_0/T_c

The function $f(T_0/T_c)$ is plotted against $\overline{K_{osc}}/K_0$ in fig. 12 for an oscillating flow with linear velocity profile between two parallel plates. For $T_0/T_c > 1$, the averaged dispersion coefficient becomes independent of the ratio T_0/T_c and is about half the value of the dispersion coefficient in the 'corresponding' steady flow having $u_0 = \hat{u}$. Fischer (1979) states that this figure may be used to predict dispersion during tidal flow in an estuary with little or no surface elevation, but emphasises that dispersion mechanisms other than shear flow are not accounted for in fig. 12.
The nature of the non-averaged dispersion coefficient in such a flow can be expressed as:

$$K_{osc} = K_0 + f_1 \cos(2wt) + f_2 \sin(2wt)$$

in which: $f_{1,2}$ = functions of T_0/T_c
w = flow cycle frequency = $2\Pi/T_0$

Fischer 1979

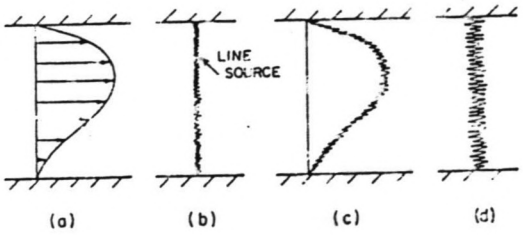

Figure 11 The shear effect in oscillating flow for the case $T_g \ll T_c$. (a) A hypothetical velocity distribution $u = u_0 \sin(2\pi t/T_g)$. (b) A line source introduced at $t = 0$. (c) The distribution at $t = T_g/2$. (d) The distribution at $t = T_g$.

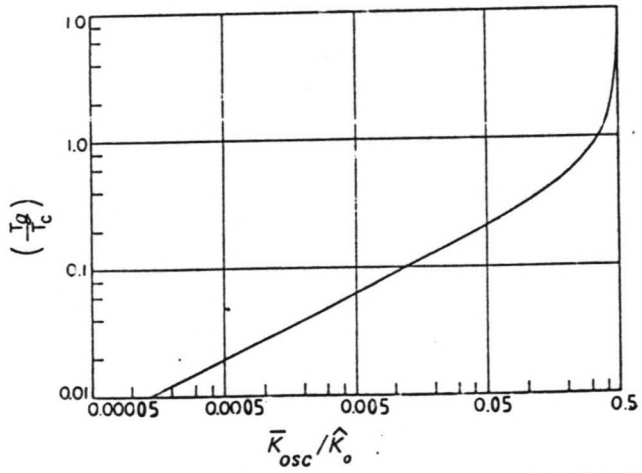

Figure 12 The dependence of the dispersion coefficient on the period of oscillation

Evidently, the non-averaged dispersion coeffcient consists of a constant part and a periodic part of twice the flow frequency. Goslinga and Verboom (1979) indicate that time averaging the dispersion coefficient over the flow cycle may be permitted after one tidal period.
Since the dispersion eq. (5) is linear, it seems possible to superimpose the results for steady and oscillating flow in order to obtain the result for the combined effect of the two flow types.
In fact, for the cycle averaged dispersion coefficient, it is:

$$K = K_0 + \overline{K_{osc}}$$

Regarding the non-averaged dispersion coefficient, however, it is not simply a matter of summing up the results. This is because a kind of non-linearity is introduced by the product of u" and ø" and because the Taylor assumptions for the steady and unsteady flow case are not the same (Goslinga and Verboom (1979)).
In fact, the combined effect of the two flow types generates interaction terms oscillating with the tidal frequency.
Flood waves, however, do not reverse, and moreover, their free surface elevation cannot be neglected. So it seems unjustified to use any of the previous results.
One important property of flood waves, however, does make it possible to use the concept of the unsteady flow results up to now.
Flood waves are, generally speaking, not as unsteady as tidal flows. Their period is often much longer than the tidal period. So the ratio T_g/T_c, although of course depending on other factors such as river geometry, has a good chance of being large, that is, much larger than unity.
Thus, dispersion during such a flow cycle can be seen as a steady state dispersion in a succession of flows that make up the cycle. In other words (from eq. (8)):

$$K(x,t) = 0.0066 \cdot \frac{u^2(x,t)B^2}{T_{yy}(x,t)} \qquad (15)$$

The flood wave period is then given by:

$$T_g/T_c = \tau \gg 1$$

in which: τ = coefficient of proportionality

So:

$$T_g = \tau \frac{B^2}{T_{yy}} = \tau \frac{B^2 \cdot C}{kau\sqrt{g}}$$

in which the relationship: $u_* = (\sqrt{g}/C) \cdot u$ is used.

Inserting this flood wave period in eq. (14) yields:

$$E = \frac{\tau^2 \cdot B^2}{kC^2 a^2 i_b^{1/2}}$$

This value of E is usually so large that the diffusion analogy gives satisfying results.
It should be noted that the dispersion equation and the diffusion analogy describe wave propagation of the same nature. The rate of damping and the propagation velocity by which the tracer cloud is directed by the dispersion equation, however, are different from damping rate and propagation velocity of a flood wave as directed by the diffusion analogy.

CHAPTER IV ANALYTICAL APPROACH

4.1 Introduction

As pointed out in Chapter III, nature is complex and mathematical models, in which nature is often already schematized to a tractable degree, often cannot be solved but for relatively simple cases. Nevertheless analytical solutions are useful, since they can provide a direct insight into their behaviour.
The dispersion equation is of parabolic type, so one initial and two boundary conditions are required. Naturally, these conditions have great influence on the solutions and they should therefore, of course, correspond with the physical environmental problem involved.
Here, solutions to the dispersion equation are, in view of constant rate discharge measurement, sought for an initial constant concentration distribution throughout the channel and a constant mass input somewhere along the channel. The channel is of constant width B.
As will be seen in Sections 2 and 3, such solutions are possible in uniform flow. Non-uniform flow, however, causes severe mathematical problems.
In Section 4 an attempt is made, after crudely simplifying the dispersion equation, to describe mixing in this flow type too.
Solutions to the flood wave equations are not given here, although these should be used to specify velocity and waterdepth appearing in the dispersion equation. As stated, there is no direct need to obtain flood wave solutions, since the flow type corresponding to such waves, is too complex to arrive at analytical solutions to dispersion during such a flow anyway.

4.2 Steady Uniform Flow Dispersion

In steady uniform flow the dispersion eq. (5) reads:

$$\frac{\delta \phi}{\delta t} + u_o \frac{\delta \phi}{\delta x} - K_o \frac{\delta^2 \phi}{\delta x^2} = 0$$

Assuming that at time t=0 there is no tracer material in the channel yields the initial condition:

$$\phi(x,0) = 0$$

One boundary condition follows from reasoning that at infinity, the concentration equals the initial concentration:

$$\lim_{x \to \pm\infty} \phi = 0$$

Mass input is a source term in the dispersion equation. In view of a one dimensional description, this mass input can be seen as mass originating from a plane source. Thus, in fact, the released substance is assumed to mix instantaneously over the cross-section. Recalling that a mass flux is given by a convective and a diffusive part, it follows:

$$(A_0 u_0 \phi - A_0 K_0 \frac{\delta \phi}{\delta x}) \Big|_{x=0} = M0(t)$$

in which: $\theta(t)$ = distribution of release in time

The Taylor method essentially corresponds to an instantaneous release, yielding:

$\theta(t)=\delta(t)$, the Dirac-delta function.

If the release is continuous, the resulting concentration distribution can be obtained using the convolution integral:

$$\phi(x,t) = \int_0^t M(t_0)\Phi(x,t-t_0)dt_0$$

in which: $\Phi(x,t-t_0)$ = concentration distribution due to an unit impulse release at $t=t_0$.

The initial length L_i and corresponding initial time T_i, during which the Taylor method does not apply, cause complications (Goslinga and Verboom (1979)).
Apart from the question whether concentration distributions found using the Taylor method differ much from the actual ones, it follows that only concentration distributions resulting from instantaneous releases before $t-T_i$ have reached a Gaussian distribution at $x>L_i$. So the convolution integral should be written as:

$$\phi(x,t)\Big|_{x>L_i} = \int_0^{t-T_i} M(t_0)\Phi_G(x,t-t_0)\Big|_{x>L_i} dt_0 + \int_{t-T_i}^{t} M(t0)\Phi_{NG}(x,t-t_0)\Big|_{x>L_i} dt_0$$

in which: Φ_G = Gaussian distributed concentration
Φ_{NG} = Non-Gaussian ditributed concentration

It now follows that the convolution integral can only be used if the contributions of the Non-Gaussian initial stage can be neglected.
It is thus assumed that the three-dimensional mixing process over the mixing length leads to concentration distributions that do not differ (much) from distributions developed after plain source injection.

This yields that the concentration distribution from a constant input with:

$\Theta(t) = H(t)$, the Heaviside-step function

can be seen as the sum of the concentration distributions resulting from impulse inputs during the time t.
So, with (fig. 1):

$$\phi(x,t) = \frac{M/A_o}{2\sqrt{(\Pi K_o t)}} \exp\left[-\left(\frac{x-u_o t}{2\sqrt{(K_o t)}}\right)^2\right]$$

as the solution for an impulse input at x=0,t=0 (e.g. de Vries (1984)), it follows that:

$$\phi(x,t) = \int_0^t \frac{M/A_o}{2\sqrt{(\Pi K_o \tau)}} \exp\left[-\left(\frac{x-u_o \tau}{2\sqrt{(K_o \tau)}}\right)^2\right] d\tau$$

is the solution for a constant input from t=0 at x=0.
This integral can be written as (Abramowitz and Stegun (1965)):

for x>0:

$$\phi(x,t) = \frac{M}{2A_o u_o}\left[\operatorname{erf}\left(\frac{u_o t-x}{2\sqrt{(K_o t)}}\right) - 1 + \exp\left(\frac{u_o x}{K_o}\right)\cdot\left(\operatorname{erf}\left(\frac{x+u_o t}{2\sqrt{(K_o t)}}\right) + 1\right)\right]$$

for x<0:

$$\phi(x,t) = \frac{M}{2A_o u_o}\left[\operatorname{erfc}\left(\frac{x-u_o t}{2\sqrt{(K_o t)}}\right) - \exp\left(\frac{u_o x}{K_o}\right)\cdot\operatorname{erfc}\left(\frac{x+u_o t}{2\sqrt{(K_o t)}}\right)\right]$$

in which: $\operatorname{erf}(z) = \frac{2}{\sqrt{\Pi}}\int_0^z \exp(-\sigma^2)\,d\sigma$

$$\operatorname{erfc}(z) = 1-\operatorname{erf}(z)$$

This solution is shown in fig. 2 for different times t. The resulting upstream transport may not be realistic from a physical point of view, since the major part of the dispersion is caused by differential convection, which only occurs in the flow direction. The only physical transport able to produce an upstream transport is turbulent diffusion which is of minor importance.
In this respect, a boundary condition at x=0 allowing only downstream transport would be more satisfactory.

de Vries 1984

$$\hat{x} = \frac{x-ut}{M/A}$$

$$\hat{t} = \frac{Kt}{(M/A)^2}$$

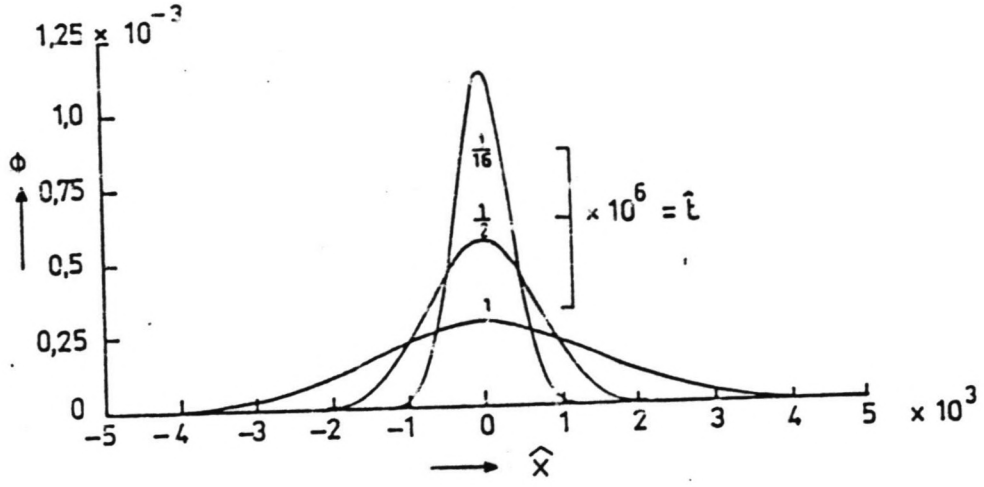

fig 1 ϕ

Berkhoff 1973

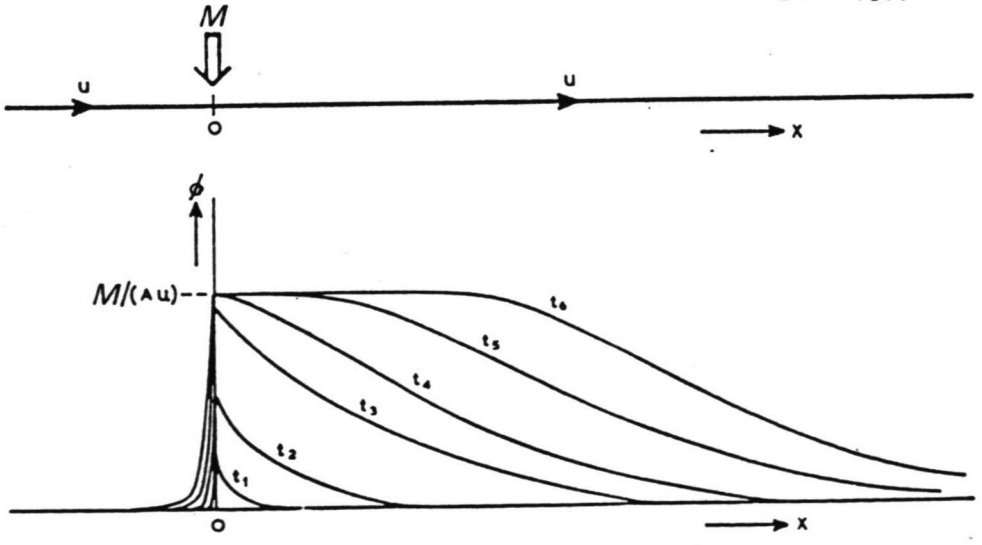

Fig 2 Concentration Distribution in the Channel.

Such a boundary condition would be:

$$\frac{\delta \phi}{\delta x} = 0 \text{ at } x=0$$

by which the mass flux condition is reduced to:

$$A_o u_o \phi \Big|_{x=0} = MH(t)$$

The solution now is given by (e.g. Fischer (1979)):

$$\phi(x,t) = \frac{M}{2A_o u_o}\left[\operatorname{erfc}\left(\frac{x-u_o t}{2\sqrt{(K_o t)}}\right) + \exp\left(\frac{u_o x}{K_o}\right)\cdot\operatorname{erfc}\left(\frac{x+u_o t}{2\sqrt{(K_o t)}}\right)\right]$$

Comparison shows that the upstream concentration is now larger by:

$$D\phi(x,t) = \frac{M}{A_o u_o}\left[\exp\left(\frac{u_o x}{K_o}\right)\cdot\operatorname{erfc}\left(\frac{x+u_o t}{2\sqrt{(K_o t)}}\right)\right]$$

in which: $D\phi$ = difference in concentration

Both solutions show that when the equilibrium state is reached for $t\to\infty$, the concentration throughout the channel for $x>0$ is:

$$\phi_o = \frac{M}{A_o u_o} = \frac{M}{Q_o}$$

which is the dilution method eq. (1) used for determining discharges after a constant rate injection.
Setting a dimensionless time $T_d = t/T_c$ and a corresponding dimensionless distance $X_d = x/(u_o T_c)$ (cf. Chapter III), yields, from inserting these parameters in the concentration distribution, that the concentration $\phi(X_d, T_d)$ is within 95% of the equilibrium value M/Q_o at a point X_d for values of T_d given in fig. 3.
It follows that in most practical cases ($X_d \approx 0.4$) some 35% of extra time above the convective time x/u_o is needed before the equilibrium state is, approximately, reached.

4.3 Unsteady Uniform Flow Dispersion

In unsteady uniform flow, the dispersion eq. (5) reads:

$$\frac{\delta \phi}{\delta t} + u_o(t)\frac{\delta \phi}{\delta x} - K_o(t)\frac{\delta^2 \phi}{\delta x^2} = 0$$

Analytical solutions could only be given here for unsteady flow of constant depth (negligible water surface elevation).

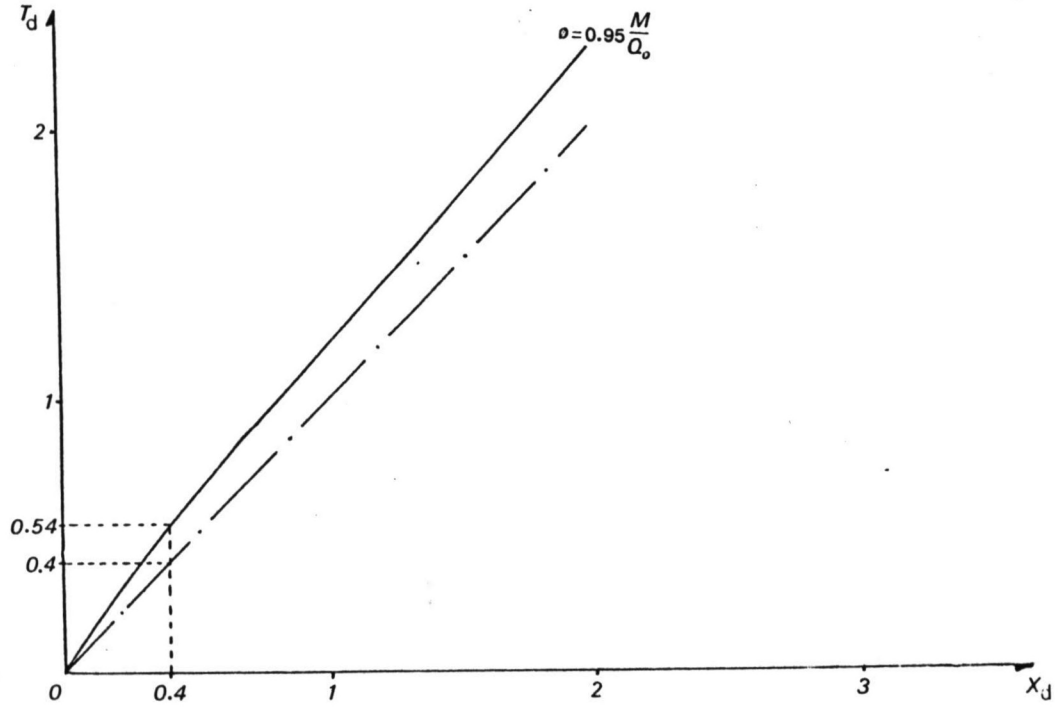

Fig 3 *Equilibrium development*

For an impulse input at t=0,x=0 the solution is given by (e.g. Goslinga and Verboom(1979)):

$$\phi(x,t) = \frac{M/A_0}{2\sqrt{(\pi \int_0^t K_0 d\tau)}} \exp\left[\left[-\frac{x - \int_0^t u_0 d\tau}{2\sqrt{(\int_0^t K_0 d\tau)}}\right]^2\right]$$

For a constant input, using the convolution integral, it follows that for a release from t=0 at x=0:

$$\phi(x,t) = \int_0^t \frac{M/A_c}{2\sqrt{(\pi \int_0^t K_0 d\tau)}} \exp\left[\left[-\frac{x - \int_0^t u_0 d\tau}{2\sqrt{(\int_0^t K_0 d\tau)}}\right]^2\right] d\tau$$

A solution allowing no upstream mixing at the point of injection could not be given here.

4.4 Unsteady Non-Uniform Flow Dispersion

In unsteady non-uniform flow the dispersion equation (5) reads:

$$\frac{\delta\phi}{\delta t} + u(x,t)\frac{\delta\phi}{\delta x} - \frac{1}{a(x,t)}\frac{\delta}{\delta x}\left[a(x,t)K(x,t)\frac{\delta\phi}{\delta x}\right] = 0$$

A general solution to this equation is not available.
A common practice in sanitary engineering has been to neglect the influence of dispersion. In the following, this procedure will be used to predict at least some aspects of spreading during an unsteady non-uniform flow.

4.4.1 A Convective Model

Crudely neglecting dispersion yields the simple wave equation:

$$\frac{\delta\phi}{\delta t} + u(x,t)\frac{\delta\phi}{\delta x} = 0$$

An order of magnitude analysis can be used to indicate when the use of this equation is justified.
Rewriting the dispersion coefficient (6), for a mean value k=0.6, as:

$$K = 0.011 \frac{C \cdot uB^2}{\sqrt{g \cdot a}}$$

yields the following dispersion equation:

$$\frac{\delta\phi}{\delta t} + u\frac{\delta\phi}{\delta x} - \frac{1}{a}\frac{\delta}{\delta x}\left[0.011\cdot\frac{C}{\sqrt{g}}B^2u\frac{\delta\phi}{\delta x}\right] = 0$$

Making the following substitution:

$$z = \bar{Z}\cdot\tilde{z}$$

in which: $\tilde{z}$ = dimensionless variable with order of magnitude of unity
$\bar{Z}$ = constant with order of magnitude of z
z = variable

yields as orders of magnitude of the three terms above:

$$\frac{\bar{\Phi}}{\bar{T}} : \frac{\overline{U\Phi}}{\bar{L}} : 0.011\cdot\frac{CB^2\overline{U\Phi}}{\sqrt{g}\cdot\overline{AL^2}}$$

or, with $\bar{U} \approx \bar{L}/\bar{T}$ and $0.011\cdot C/\sqrt{g} \approx 0.1$

$$1 : 1 : 0.1\cdot\frac{B^2}{\bar{A}\cdot\bar{L}}$$

Setting:

$$0.1\cdot B^2/\overline{A\bar{L}} = \tau << 1 \quad \text{or} \quad B^2/\overline{A\bar{L}} << 10$$

yields:

$$\frac{\delta\tilde{\phi}}{\delta\tilde{t}} + u\frac{\delta\tilde{\phi}}{\delta\tilde{x}} - \tau\frac{1}{\tilde{a}}\frac{\delta}{\delta\tilde{x}}\left[\tilde{u}\frac{\delta\tilde{\phi}}{\delta\tilde{x}}\right] = 0$$

From an asymptotic procedure:

$$\phi = \sum_{j=0}^{n} \tau^j \phi_j + O(\tau^{n+1})$$

in which: $\phi_j = \frac{1}{j!} \cdot \frac{\delta^j \phi}{\delta \tau^j}$

it follows:

$$\frac{\delta \phi_0}{\delta t} + u \frac{\delta \phi_0}{\delta x} + \tau \left[\frac{\delta \phi_1}{\delta t} + u \frac{\delta \phi_1}{\delta x} - \frac{1}{a} \frac{\delta}{\delta x} \left(u \frac{\delta \phi_0}{\delta x} \right) \right] + \ldots +$$

$$+ \tau^n \left[\frac{\delta \phi_n}{\delta x} + u \frac{\delta \phi_n}{\delta x} - \frac{1}{a} \frac{\delta}{\delta x} \left(u \frac{\delta \phi_{n-1}}{\delta x} \right) \right] + O(\tau^{n+1})$$

So it follows that for a zero-th order approximation only, the concentration is given by the simple wave equation:

$$\phi = \phi_0 + O(\tau)$$

with ϕ_0 following from: $\frac{\delta \phi_0}{\delta t} + u \frac{\delta \phi_0}{\delta x} = 0$

The ratio $B^2/\overline{AL}$ consists of characteristic lengths.

B is the river width B.

$\overline{A}$ can be seen as the river depth a.

The nature of the approximation used is that it only holds for slowly varying circumstances. Concentration distributions resulting from an instantaneous release can therefore not be computed using the simple wave approach. For a continuous constant release, it thus follows:

$\overline{L}$ can be seen as the flood wave length L_g

This yields that the approximation can be used ($\tau \ll 1$) if:

$$\frac{B^2}{aL_g} \ll 10$$

An estimate of the error made when using this zero-th order approximation follows from realising that dispersive transport is neglected compared to the convective transport. So:

$$F = \left[\frac{K \delta \phi / \delta x}{u \phi} \right]$$

in which: F = relative error

4.4.2 A Constant Input Solution

Solving a simple wave equation requires one initial and one upstream boundary condition.
So, together with the familiar initial condition:

$$\phi(x,0) = 0$$

and a boundary condition:

$$\phi(o,t) = \phi(t)$$

the problem is defined.
The method followed to obtain a solution is the method of characteristics and the problem as defined above is a classical boundary value problem (e.g. Whitham (1974)).
The characteristics in the x-t plane of the simple wave equation are:

$$\frac{dx}{dt} = u(x,t) \quad \text{with} \quad \frac{d\phi}{dt} = 0 \quad \text{along them.}$$

So a value of ϕ given at a certain time t_o at the upstream boundary remains constant in time and place along the characteristic that intersects the boundary at $t=t_o$.
By varying the parameter t_o, all values of ϕ given at the boundary can be seen 'transported' along all characteristics intersecting the boundary and so a solution for ϕ is given (fig. 4).
Of course, the possibility of actually expressing ϕ in x and t depends on the complexity of the functions involved.
Assuming the following relationships for velocity and waterdepth (for $t > x/c$):

$$u = u_o + \alpha(t-x/c)$$
$$a = a_o + \beta(t-x/c)$$

in which: α, β, c are constants, yields:

$$\frac{dx}{dt} = u_o + \alpha(t-x/c)$$

so:

$$x = C_1 \cdot \exp\left(-\frac{\alpha}{c}t\right) + ct + \frac{c}{\alpha}(u_o - c)$$

Intersecting the boundary x=0 at $t=t_o$ yields a typical characteristic in the x-t plane:

$$\frac{x}{c} = t + \frac{1}{\alpha}(u_o - c) - \left[t_o + \frac{1}{\alpha}(u_o - c)\right] \cdot \exp\left[-\frac{\alpha}{c}(t - t_o)\right]$$

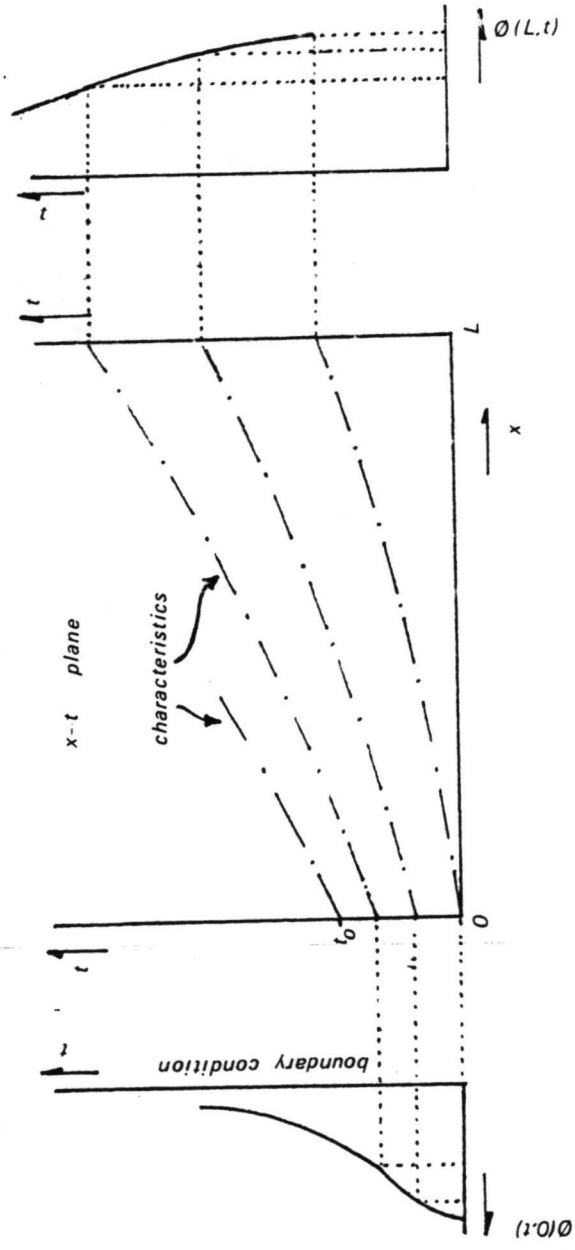

Fig 4 Integration by characteristics

This characteristic 'transports' a boundary value:

$$\phi(0,t_0) = \frac{M/B}{a(0,t_0)u(0,t_0)}$$

Elimination of t_0 now yields:

$$x = f(\phi,t)$$

by which ϕ is (implicitly) given.

For slowly varying circumstances, the boundary condition may be written as (neglecting higher order terms in α and β):

$$\phi(0,t_0) \approx \frac{M/B}{a_0u_0 + (a_0\alpha + u_0\beta)t_0}$$

and so ϕ is given by:

$$\frac{x}{c} \approx t + \frac{1}{\alpha}(u_0-c) - \left[\frac{M/B\phi - a_0u_0}{a_0\alpha + u_0\beta} + \frac{1}{\alpha}(u_0-c)\right]\exp\left[-\frac{\alpha}{c}(t - \frac{M/B\phi - a_0u_0}{a_0\alpha + u_0\beta})\right]$$

In Chapter VI this simple wave approximation will be used to support the computational results.

CHAPTER 5 NUMERICAL APPROACH

5.1 Introduction

A vast amount of computational methods on both open channel flow and dispersion is available. Quoting from Vreugdenhil (1982):
'However, searching for an optimal method does not seem very useful: the important thing is to avoid an uncritical use of any numerical model.'
clearly defines the numerical approach. A newly developed model (Urbanus and Vreeburg (1987)) has been used, after extension, for this study.
The model uses a finite difference appraoch. The solution is found at successive time levels: starting from the previously computed solution at a time t, a step is made to the next time level t+Dt.
The model is implicit. In an explicit model, the unknown variables at a computational point are (generally) directly determined from variables all known by computation at the previous time level. In an implicit model, in addition, other still unknown variables from the same time level are used. Thus a system of relations between these unknown variables still remains to be solved (fig. 1).
Although this complicates the computation, implicit models have the advantage that, under certain conditions, with respect to stability no restrictions concerning the time step are imposed. Explicit models generally turn out to be stable only if the speed with which information travels in the numerical scheme is faster that the physical speed of propagation of a disturbance (fig. 2).
Concerning accuracy, however, it should be realised that mesh width and time step must be in reasonable relation to the length and time scales involved in the problem at hand. Furthermore, desired accuracy is strongly related to the specific use of a computation. Both points are discussed in Section 4.
As with an analytical approach, initial and boundary conditions are needed to start a computation and solve the difference equations. These are treated in Section 3.
Firstly, the finite difference schematization used, is discussed in Section 2.

5.2 Channel Schematization

The numerical model represents a channel as a series of storage basins connected by conduits with friction and inertia (fig. 3). The channel is rectangular and of constant width.
At a storage basin (a 'node') the equation of continuity is applied, stating that the net inflow is balanced by a rise or fall in the water level. At the conduits ('branches') the momentum equation is applied and the discharge is computed at the boundaries between adjacent nodes.
The dispersion equation is solved per node, thus having a mesh width Dx double the size of the flow equations' mesh width.

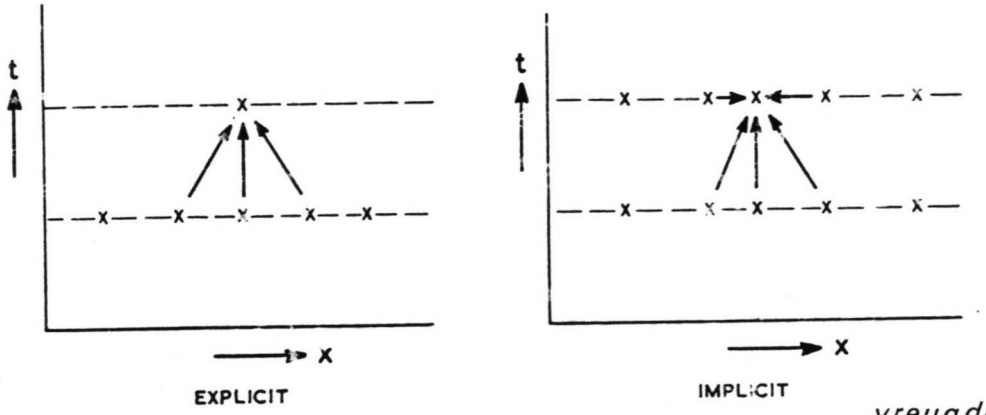

Fig. 1 Explicit and implicit methods.

vreugdenhil 1973

Fig. 2 The Courant-Friedrichs-Lewy condition for stability

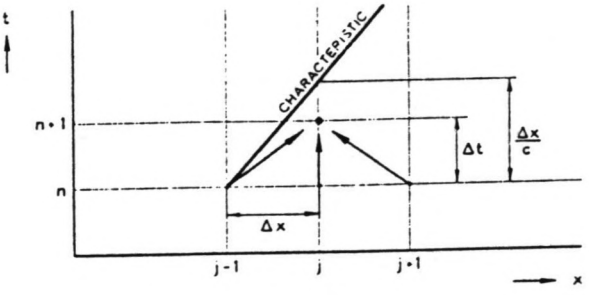

Jansen 1979

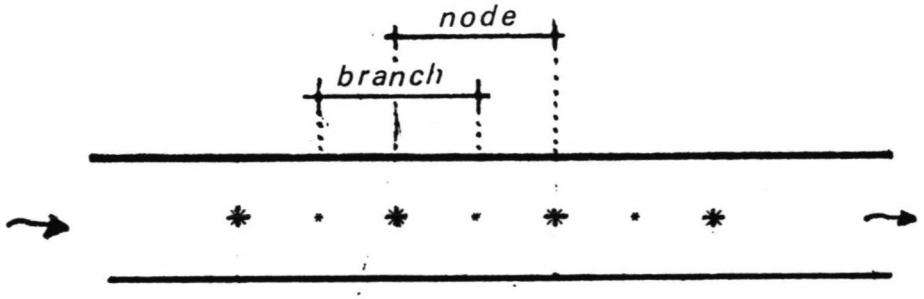

* *mesh point for waterlevel and concentration*

✱ " " " *discharge and mass flux*

Fig. 3 Example of schematization.

The difference equation for unsteady flow is dynamic and the difference scheme used is of Cranck-Nicholson type (fig. 4). To solve the flow equations they are linearised by defining e.g.:

$$a(t+Dt) = a(t) + Da$$

in which: Da = difference in e.g. depth
Dt = time step

From a known condition at time t, the variables at t+Dt are computed by computing Da, and so on. The coefficients appearing in the linearised equations are evaluated at time t.
The difference scheme for the dispersion equation is also of Cranck-Niholson type, with the mass-flux evaluated at half the mesh widths, that is, at the nodes' boundaries (fig. 4). The chosen scheme is central and both schemes use a weighing factor θ of 0.55, thereby ensuring stability and minimizing numerical diffusion (fig. 5)

5.3 Initial and Boundary Conditions

Solving the difference equation for unsteady flow, which is of hyperbolic type, requires two initial conditions (one for water-depth (waterlevel) and one for velocity (discharge)) and two boundary conditions (one at every boundary, either in velocity (discharge) or waterdepth (waterlevel), or as a relation between the two).
As an initial condition, the model starts from a steady flow condition, using the Chezy relationship.
At the upstream boundary, a flood wave discharge is specified having a Gaussian distribution (fig. 6):

$$Q(0,t) = Q_0 + \hat{Q}\exp\left[-\tfrac{1}{2}\left(\frac{t-\tau}{\sigma}\right)\right]^2$$

in which: $\hat{Q}$ = discharge amplitude
τ = time to peak discharge
σ = wave's standard deviation

At the downstream boundary, Jones' formula is used. This is a local application of the kinematic wave approach to the diffusion analogy (e.g. Verspuy and de Vries (1981)). With:

$$g\frac{\delta a}{\delta x} - gi_b + g\frac{u^2}{C^2 a} = 0$$

and:

$$\frac{\delta a}{\delta t} + \frac{3}{2}u\frac{\delta a}{\delta x} = 0$$

Fig. 4 Arrangement of mesh points

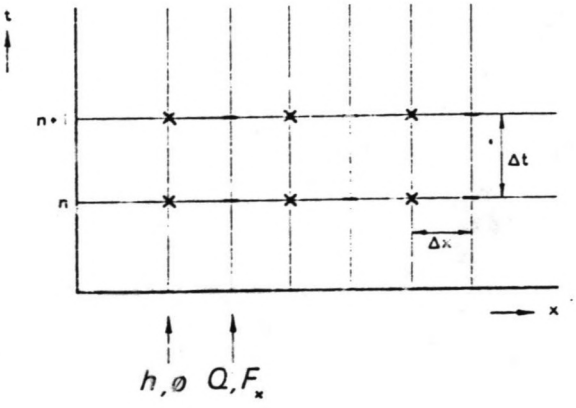

Fig. 5 Significance of parameter θ

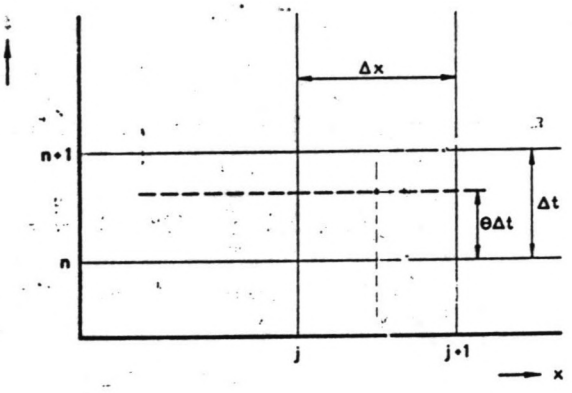

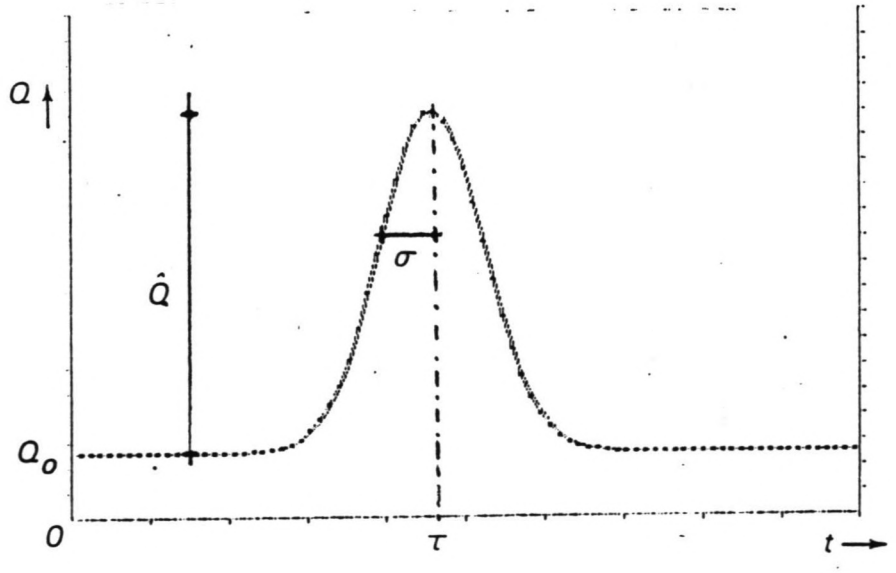

Fig 6 Gaussian flood wave

it follows that:

$$\frac{\delta a}{\delta t} = c\left(\frac{u^2}{C^2 a} - i_b\right)$$

which is the Jones' formula.

in which: c = propagation velocity = $\frac{1}{B}\frac{dQ}{da}$ for constant C.

$$= \frac{3}{2} u \text{ per unit width}$$

Contrary to a stage-discharge relationship, as given by the Chezy relationship, Jones' formula accounts for the loop effect in the flood wave's rating curve (fig. 7).
In the implicit scheme Jones' formula reads, in waterlevel and discharge fashion:

$$\frac{h^{n+1}-h^n}{Dt} = \theta\left[c\,\frac{1}{C^2RA^2}\,Q^2 - ci_b\right]^{n+1} + (1-\theta)\left[c\,\frac{1}{C^2RA^2}\,Q^2 - ci_b\right]^{n}$$

in which: h = waterlevel
R = hydraulic radius
n = number of time steps
θ = weighing factor

Linearisation of h and Q and approaching the coefficients in a Taylor series with respect to n+θDt yields:

$$h^{n+1} = h^n + Dh$$
$$Q^{n+1} = Q^n + DQ$$

$$c^{n+1} = c^n + \theta\,\frac{dc}{dh}Dh + \ldots.$$

$$\frac{1}{C^2RA^2}^{n+1} = \varepsilon^{n+1} = \varepsilon^n + \theta\,\frac{d\varepsilon}{dh}Dh + \ldots.$$

Inserting these yields:

$$Dh\left[\frac{1}{Dt} - \theta^2 c^n\frac{d\varepsilon}{dh}Q^nQ^n - \theta^2\varepsilon^n\frac{dc}{dh}Q^nQ^n + \theta^2\frac{dc}{dh}i_b\right] + DQ\left[-2Q^n\varepsilon^n c^n\theta\right] =$$

$$= c^n\varepsilon^nQ^nQ^n - c^n i_b$$

Now this equation is solved at the downstream boundary instead of the continuity equation. The propagation speed is taken according to the diffusion analogy (Jansen (1979)):

$$c = \frac{1}{B}\frac{dQ}{da} = \frac{Q}{B}\left[\frac{1}{C}\frac{dC}{dh} + \frac{1}{A}\frac{dA}{dh} + \frac{1}{2R}\frac{dR}{dh}\right]$$

Fig. 7 Loop in rating curve for flood wave
1 – local maximum for velocity
2 – local maximum for discharge
3 – local maximum for depth = flood maximum for discharge
4 – flood maximum for depth

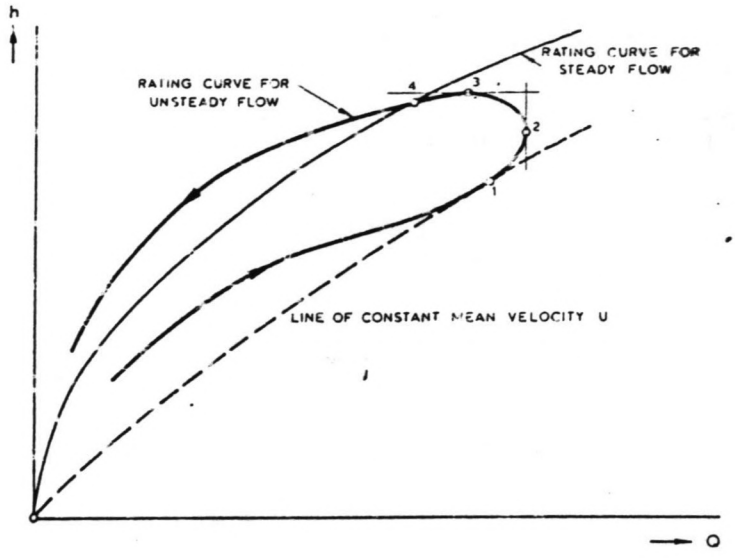

Jansen 1979

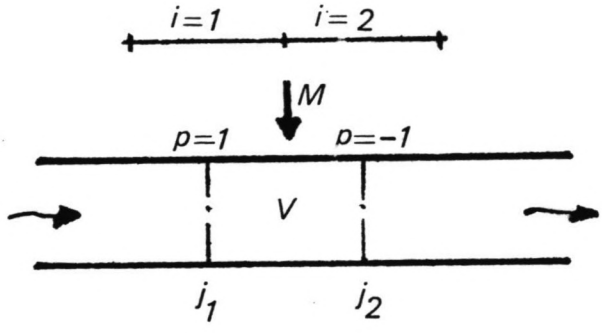

Fig. 8 Scheme of a Node.

Solving the difference equation for dispersion, requires (Chapter IV) one initial and two boundary conditions.
As an initial condition the model starts with zero background concentration throughout the channel.
At the upstream boundary mass input is specified as a source term in the dispersion equation. In volume fashion the dispersion equation then reads (fig. 8):

$$\frac{\delta V\phi}{\delta t} + \sum_{i=1}^{m} p\left[Au\phi - AK \frac{\delta \phi}{\delta x} \right]_j = M$$

in which: V = volume of the node
m = number of branches connected with the node
p = indicator whether a branch discharges to or from a node
j = specific boundary with adjacent nodes

At the downstream boundary the model uses $\delta\phi/\delta x=0$ as a boundary condition, so no dispersive transport is assumed (Chapter IV). Upstream dispersion at the node of release is avoided in the same way.

5.4 Accuracy

5.4.1 Introduction

The results of a computation have little or no value if nothing can be said about their accuracy. Giving a precise prediction of a result's accuracy is, however, not easy and often not even possible.
This is, firstly, because many sources of inaccuracy are incorporated in the final result of a computation.
Secondly, because the precise error magnitude of the contributions of these error sources is often not known.
Thirdly, because the combined effect of these error sources often cannot be predicted.
Some error sources have already been stipulated. The discrepancy between nature and mathematics, the inaccuracy of physical data (e.g. dispersion coefficients or roughness) or even the incorrect use of a model (e.g. using a simple wave model when its approach is not justified).
This section is concerned with errors due to numerical effects.

5.4.2 Flood Waves

Damping and propagation of a wave (fig. 9) can be represented differently in a numerical computation (fig.10).
The propagation velocity may be too large or too small and the damping may also differ due to numerical effects.
The desired accuracy of representation will yield a desirable

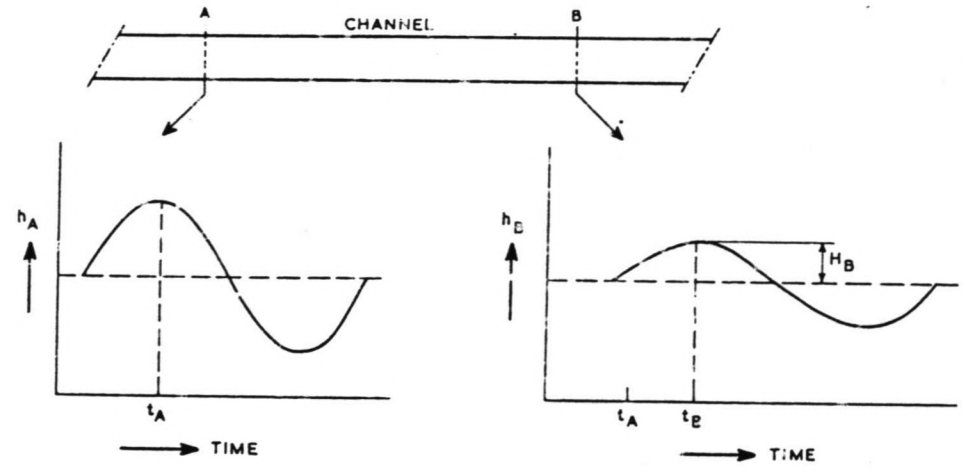

Fig. 9 Wave propagation.

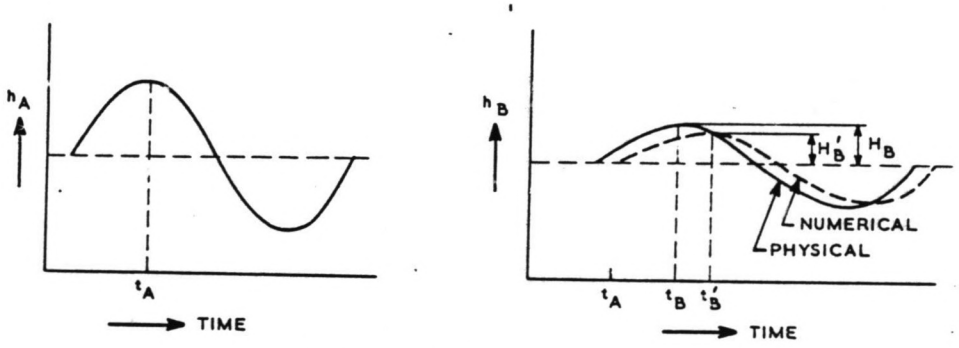

Fig. 10 Numerical wave propagation.

vreugdenhil 1973

mesh width and time step for running a computation. The influence of the weighing factor θ is disregarded here, since it is fixed at 0.55 in the model at hand.
A quantitative method for choosing Dx and Dt is given by Vreugdenhil (1985).
With respect to a wave that is not damped by friction, the following ratios between numerical and analytical damping and propagation velocitiy can be given:

$$d_n = |\Gamma|^n = \text{damping factor per wave period}$$

$$c_r = \frac{\arg(\Gamma)}{2k_0 cDt} = \text{relative celerity per wave period}$$

in which: n = number of time steps per wave period
$k_0 = 2\Pi/L_0$ = wave number
Γ = amplification factor of the numerical scheme

Fig. 11 gives values of d_n and c_r for different Dx and Dt and θ=0.55. In an ideal situation, both d_n and c_r would be unity. The influence of friction may be analysed considering the differential equation:

$$\frac{\delta Q}{\delta t} + rQ = 0$$

and its difference approximation:

$$\frac{Q_j^{n+1} - Q_j^n}{Dt} + r\left[\theta Q_j^{n+1} - (1-\theta)Q_j^n\right] = 0$$

in which: r = friction factor = $2\,\frac{g}{C^2}\,\frac{Q_0}{a_0 A_0}$

For an initial condition $Q(x,0) = Q_0$ the solutions to both equations above are given by:

$$Q(t) = Q_0 \exp(-rt)$$

$$Q(t) = Q_0\left[\frac{1-(1-\theta)rDt}{1+\theta rDt}\right]^{t/Dt}$$

Now consider the relaxation time t_e=1/r. If the analytical and numerical computation would give equal results, it would follow that:

$$\left[\frac{1-(1-\theta)rDt}{1+\theta rDt}\right]^{t_e/Dt} = 1/e$$

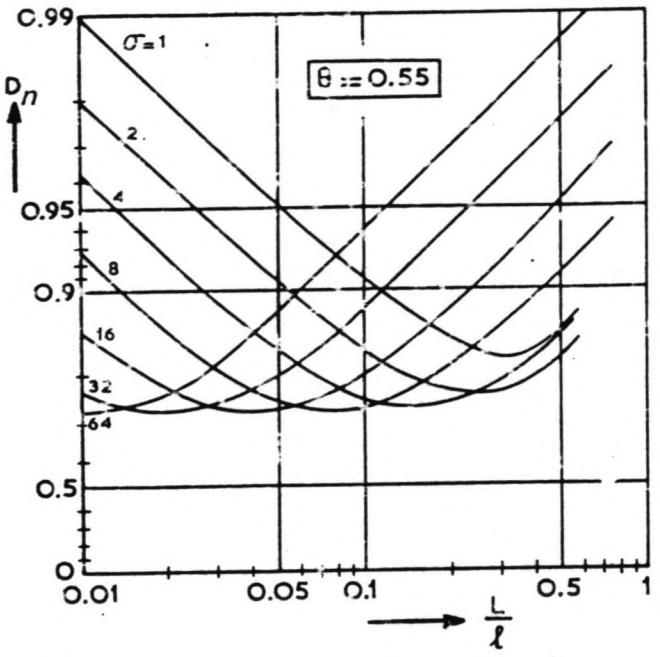

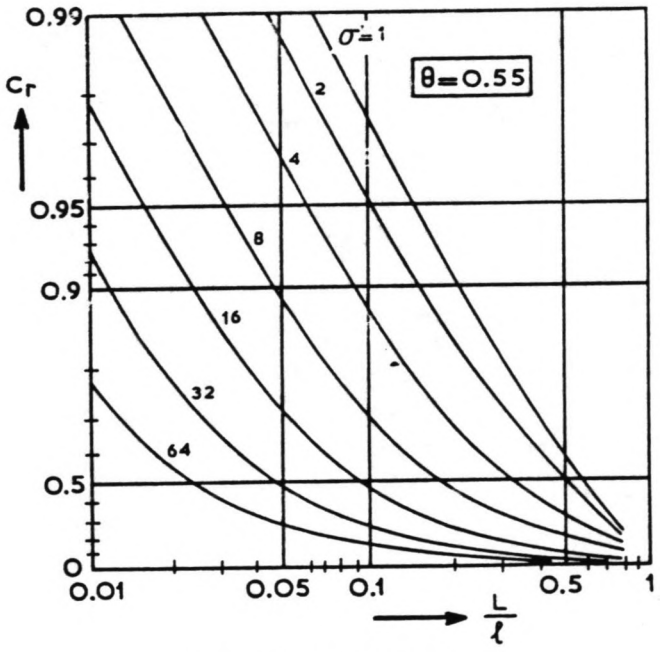

Fig. 11 Numerical effects.
L = branch length, l = wave length, $\sigma = 2c\Delta t/L$.

vreugdenhil 1973

($L = \Delta x$)

Since, however, there will be a discrepancy between both solutions, a damping factor d_r can be defined as:

$$d_r = \frac{-rDt}{\ln\left[\frac{1-(1-\theta)rDt}{1+\theta rDt}\right]}$$

Fig. 12 gives d_r as a function of rDt for θ=0.55.

When separate analyses of both mechanisms described yield satisfactory results, it may be expected that their combined effect will be satisfying too (Vreugdenhil (1985)).

5.4.3 Dispersion

Accuracy in representing the dispersion process is determined by effects as numerical dispersion, occurrence of spacial oscillation, and the effects of both the convective and the diffusive mechanism.
When separate analyses into these effects yield reasonable accuracy for a given Dx, Dt and θ, it may, again, be expected that the accuracy as a whole is acceptable (Vreugdenhil (1985)).

Numerical dispersion caused by the difference scheme can be quantified expanding each difference term in a Taylor series. This yields the 'modified' equation. For a central scheme (e.g. Vreugdenhil (1985)):

$$\frac{\delta\phi}{\delta t} + u\frac{\delta\phi}{\delta x} - K\frac{\delta^2\phi}{\delta x^2} = -\tfrac{1}{2}(1-2\theta)Dt\frac{\delta^2\phi}{\delta t^2} + O(Dx^2, Dt^2)$$

The right hand side of this 'modified' equation is the 'truncation' error and consists of terms among which a term can be recognized with the nature of a diffusion term (e.g. Vreugdenhil (1985)):

$$K_{num} = -\tfrac{1}{2}(1-2\theta)Dt\cdot u^2$$

Apparently, the computation is carried out with an effective dispersion coefficient:

$$K_{eff} = K + K_{num}$$

This has two consequences. For reasons of stability, the effective dispersion coefficient should not be negative. This is ensured for θ=0.55. For reasons of accuracy, the numerical dispersion should be an order of magnitude smaller than the physical dispersion.
The model under consideration artificially lowers the physical dispersion coefficient, to make the effective dispersion coefficient represent the actual physical situation. It should be emphasised, however, that the other terms in the truncation error may be important as well. They are, however, more difficult to interpret.

Fig 12 Friction Influence

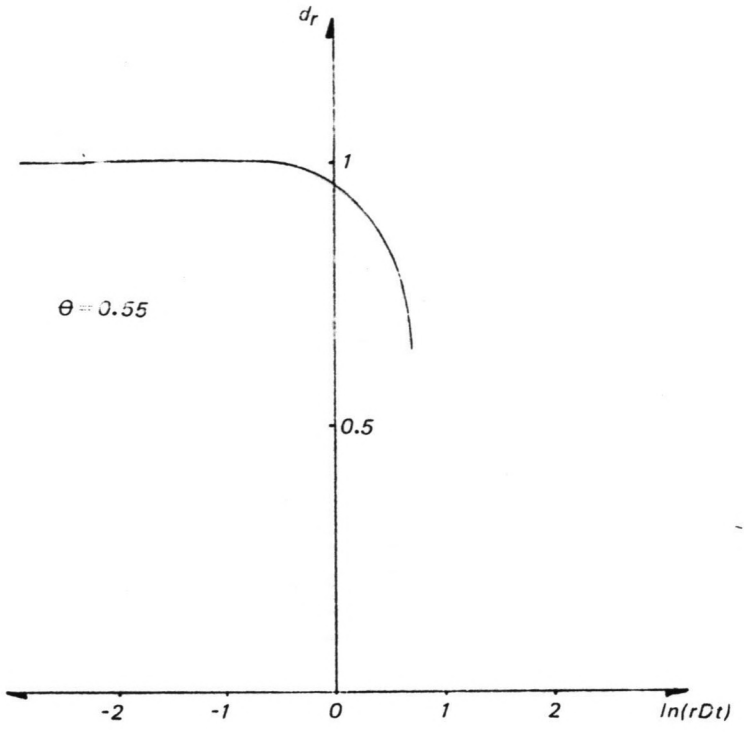

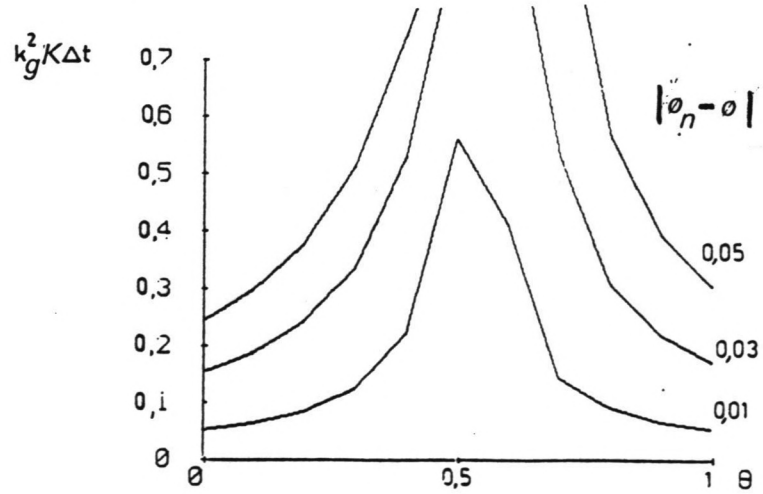

Fig 13 Diffusion Influence

vreugdenhil 1985

Fig 14 Convection Influence

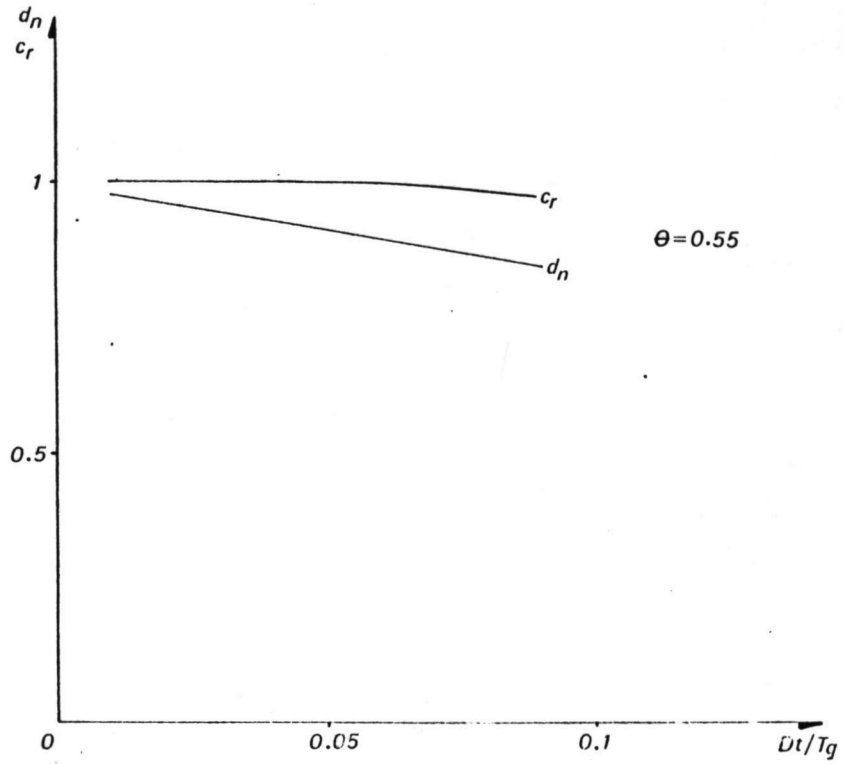

Even if a computational method is stable, oscillations can occur. The existence of these oscillations is governed by the cell-Peclet number (e.g. Vreugdenhil (1985)):

$$P = \frac{u \cdot Dx}{K}$$

in which: P = cell-Peclet number
Dx = mesh width

The source of their excitation is a sudden variation in concentration imposed by a boundary condition (e.g. a sudden release of a large amount of material). A sufficient condition to prevent these oscillations is given by (e.g. Vreugdenhil (1985)):

$$P < 2$$

The accuracy of the finite difference method for diffusion only, can be judged by considering the diffusion equation as a 'black box' which transfers a certain 'input signal' at one location to an 'output signal' at another (e.g. Vreugdenhil (1985)). The difference between the transfer functions of the differential and the difference equation during, for example, the relaxation time, yields a measure for the accuracy. This is given in fig. 13 as function of θ,K,k_o and Dt.

The influence of convection can, again, be estimated by comparing propagation and damping by the differential and difference equation. For small values of $2\Pi \cdot Dt/T_o$, the relative celerity c_n and damping factor d_n are given in fig. 14 as a function of Dt/T_o for θ=0.55.

5.4.4 Evaluation

From comparing computations with analytical solutions it may be concluded that the model produces fair results with respect to steady flow dispersion as well as flood wave representation.
It is thus assumed that the model will also produce satisfying results when computing dispersion during flood waves.

CHAPTER VI RESULTS

6.1 Introduction

In view of a practical approach to discharge measurements during unsteady flow by constant rate injection, the errors relative to measurements during steady flow are evaluated, by determining the discharge from the concentration distribution (or 'chemograph'), using the steady state relationship (eq. (2)):

$$Q_m(L,t) = \frac{M}{\phi(L,t)}$$

In the computational model, such a discharge measurement is simulated. The discrepancy between the "measured discharge" Q_m and the "actual discharge" Q_r defines the relative error:

$$\varepsilon(x,t) = \frac{Q_r(x,t)-Q_m(x,t)}{Q_m(x,t)}$$

The nature of the function ε is studied for Gaussian shaped flood waves (Chapter V) propagating down a rectangular uniform channel.

6.2 Qualitative Results

In all computations made, the behaviour of the function ε in time at a certain distance from the point of injection is typically that of fig. 1.
Several sources contribute to this behaviour.
Dispersion causes damping of the Q_m wave. Flood wave behaviour causes damping and distortion of the Q_r wave. The main source causing the oscillation in fig. 1, however, is a phase shift between the actual and the measured discharge, as is shown in fig. 2.
This phase shift is caused by the difference in propagation velocity of both waves. The Q_m wave travels with a propagation velocity somewhere between the base flow velocity u_0 and the maximum flow velocity during flood wave passage, whereas the flood wave travels with a propagation velocity about 1.5 times as large, the actual value depending on flood wave properties and river characteristics.
This yields that the time lag between both waves increases with distance from the injection point (fig. 3), which, in turn, increases the maximum errors.

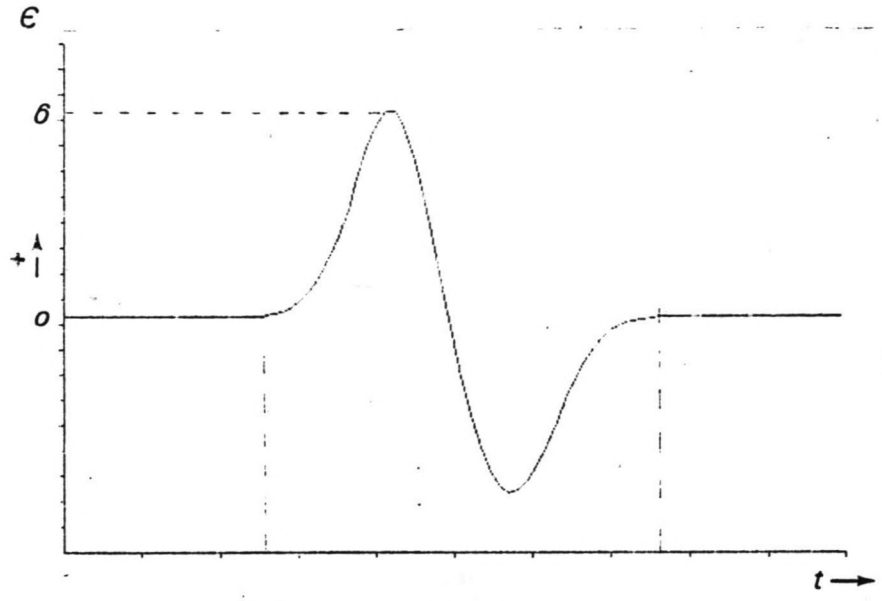

fig 1 $\epsilon(x,t)$

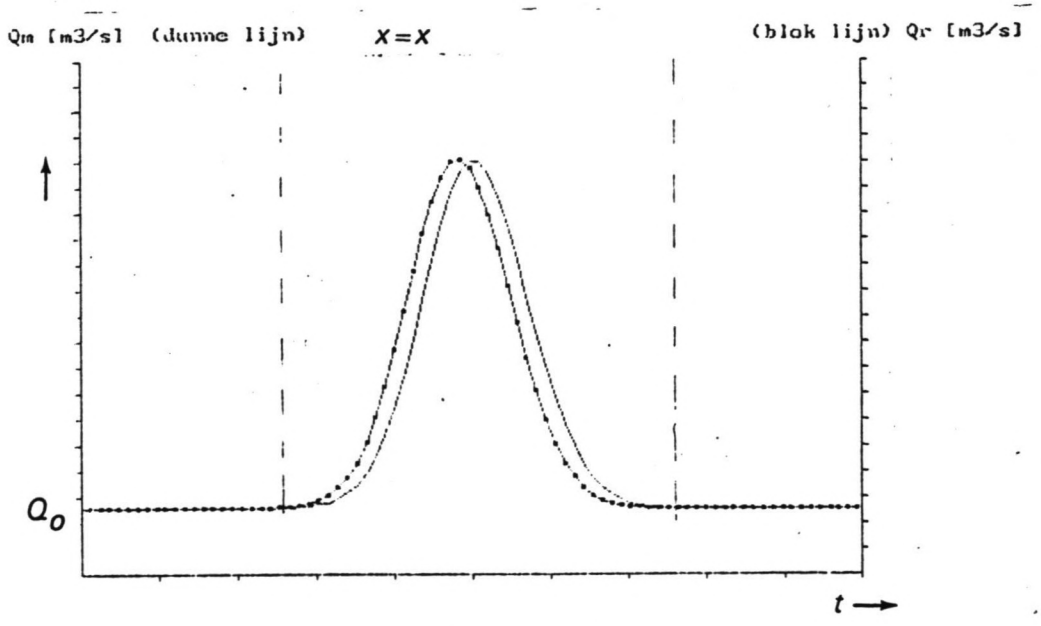

fig 2 *Phase shift*

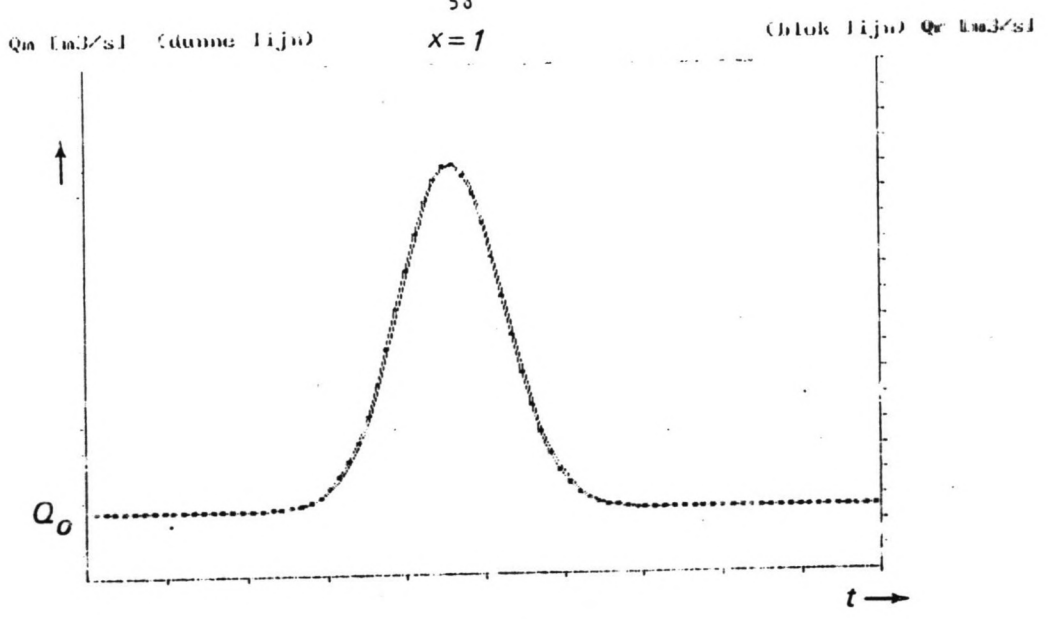

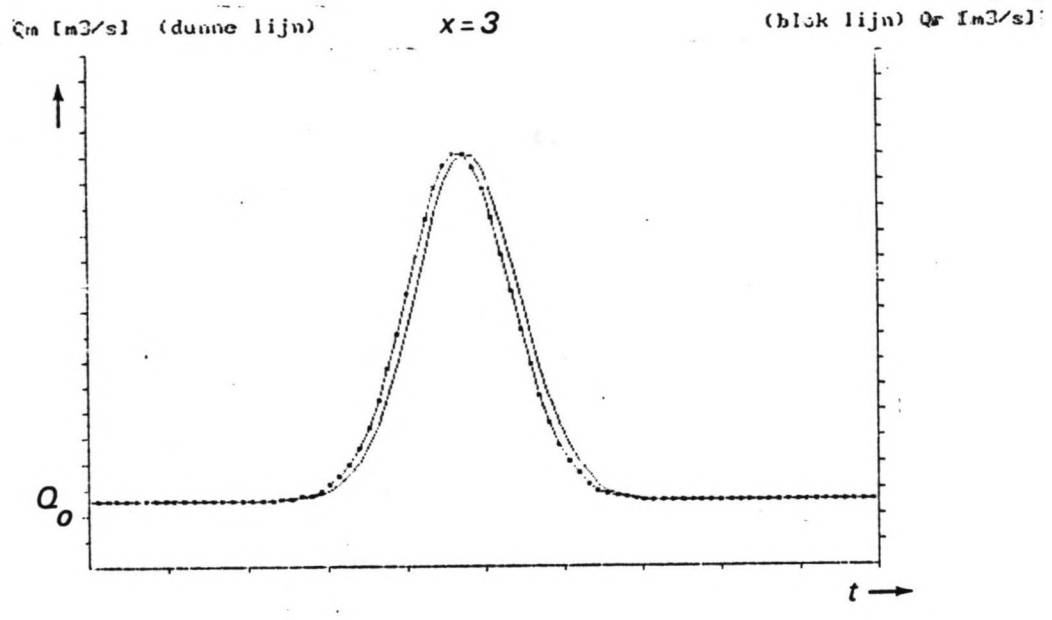

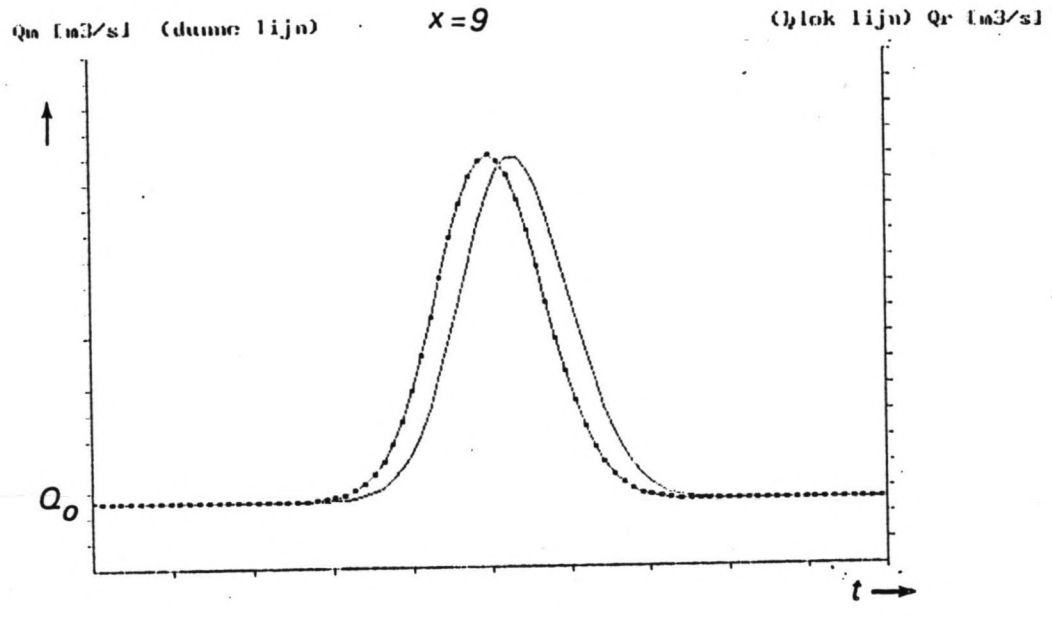

fig 3 Spatial influence

Fig 4

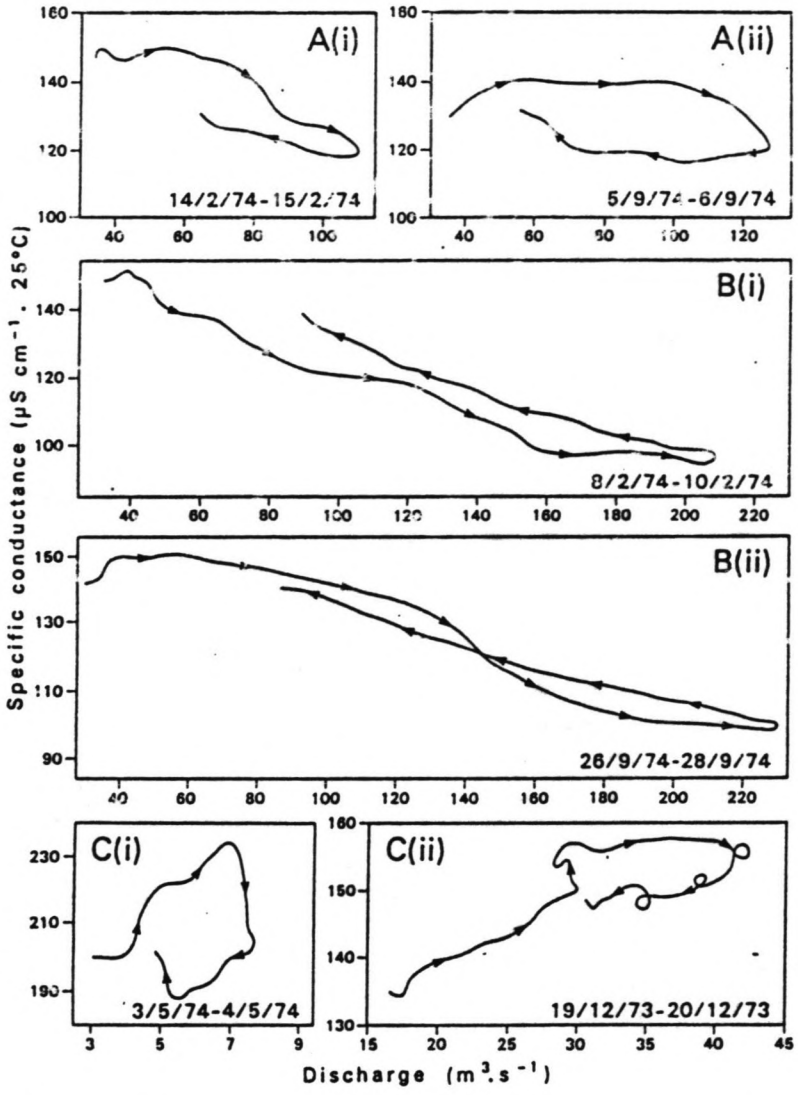

Hysteretic loops for selected individual storm runoff events for the River Exe at Thorverton.

(Walling, D.E. and Webb, B.W., 1980.)

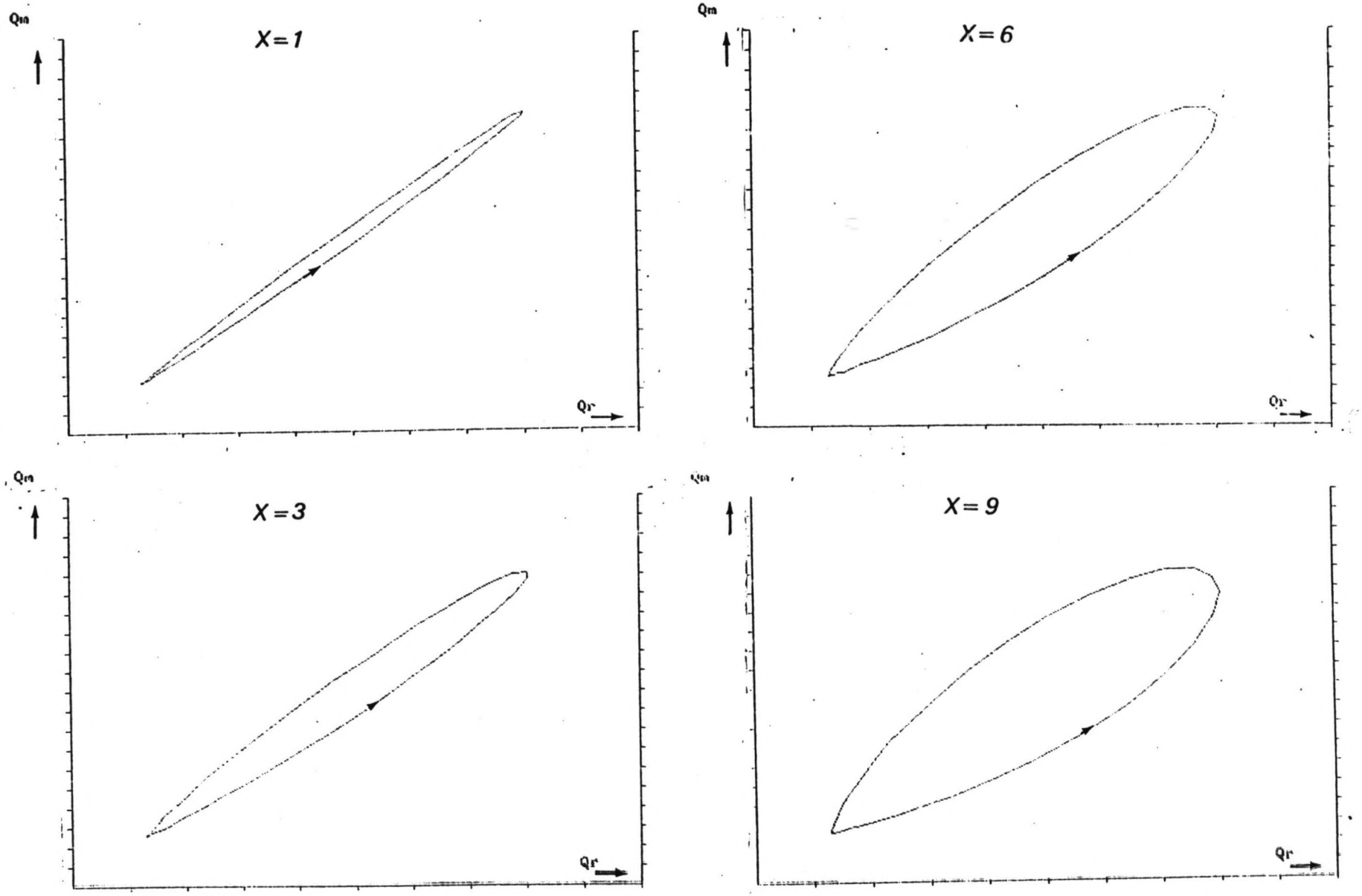

Fig 5 Hysteretic loop development

Fig 6 Phase shift influence on ε

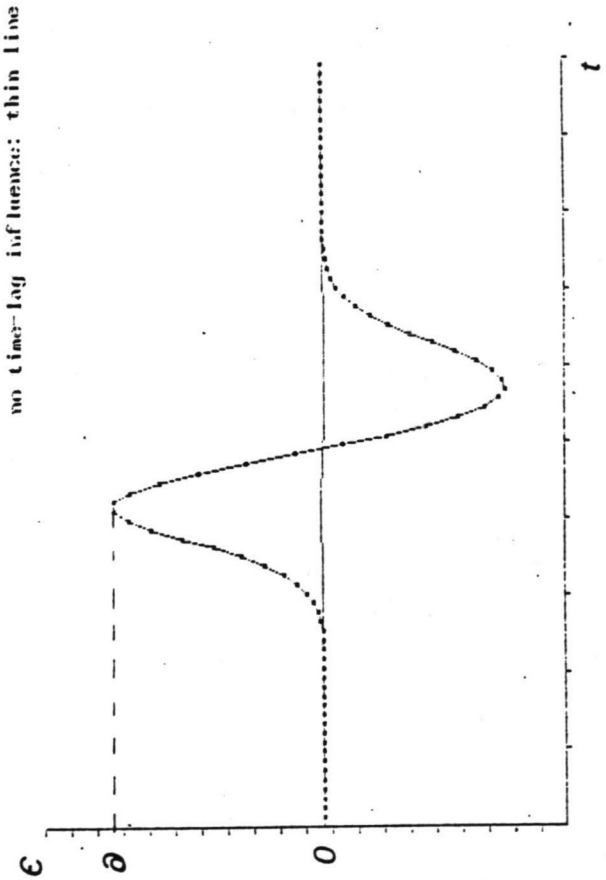

This influence of the spatial dimension on the time history of the error has been observed in laboratory and field experiments (e.g. Glover and Johnson (1974), Walling and Webb (1980), Van Craenenbroeck and Marivoet (1987)). The resulting hysteretic loop development with distance from the injection point, observed in both field experiments (fig. 4) and computations (fig. 5) typically illustrates this.
With a time lag small compared to the flood wave period, as will be the case with most discharge measurements, maximum errors occur near or at the times of maximum inertia ($\delta Q/\delta t$) and storage ($\delta a/\delta t$), while near the maximum and minimum discharges, the error is small. This is similar to observations by Kilpatrick and Cobb (1986). It should be noted, however, that these relationships are not typical, but strongly depend on the order of magnitude of the time lag compared to the flood wave period.
The influence of sources other than difference in propagation velocities of both waves may be demonstrated by artificially "reshifting" so as to cause the time lag to disappear. Comparing the thus remaining errors with the original ones, shows (fig. 6), that difference in propagation velocities is by far the most important source of error development.

6.3 Analytical background

As a means of evaluating these computational results the analytical approach in Chapter IV can be used. From that simple wave approximation it followed that for a flow having:

$$u = u_o + \alpha(t-x/c)$$
$$a = a_o + \beta(t-x/c)$$

the concentration resulting from a constant rate injection was defined by ($t > x/c$):

$$\frac{x}{c} \approx t + \frac{1}{\alpha}(u_o-c) - \left[\frac{M/B\phi - a_o u_o}{a_o\alpha + u_o\beta} + \frac{1}{\alpha}(u_o-c)\right]\exp\left[-\frac{\alpha}{c}(t - \frac{M/B\phi - a_o u_o}{a_o\alpha + u_o\beta})\right]$$

Using the steady state relationship (eq. (2) per unit width):

$$q_m = M/B\phi$$

it follows that:

$$\frac{x}{c} \approx t + \frac{1}{\alpha}(u_o-c) - \left[\frac{q_m - a_o u_o}{a_o\alpha + u_o\beta} + \frac{1}{\alpha}(u_o-c)\right]\exp\left[-\frac{\alpha}{c}(t - \frac{q_m - a_o u_o}{a_o\alpha + u_o\beta})\right]$$

Starting with a boundary condition:

$$q_m(0,t_o) \approx a_o u_o + (a_o\alpha + u_o\beta)t_o \approx q_r(0,t_o)$$

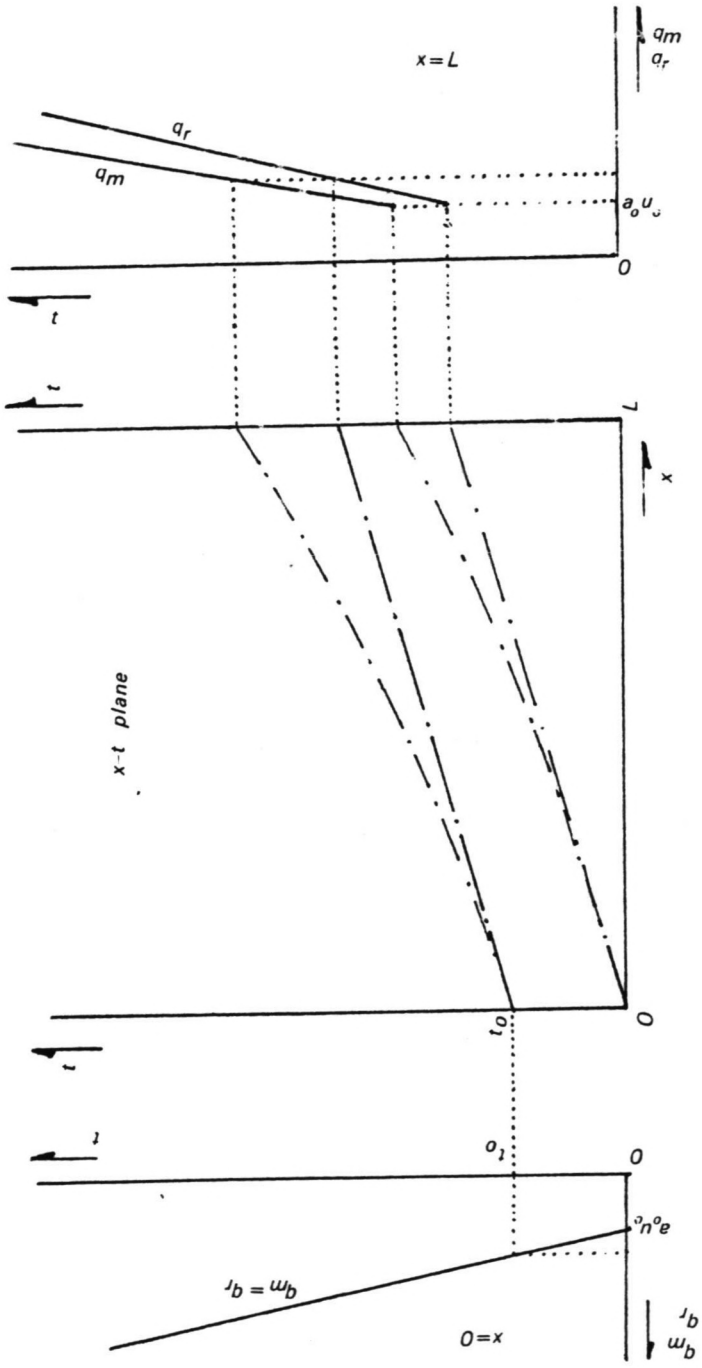

Fig 7 q_m and q_r propagation

fig 8 . error growth with distance

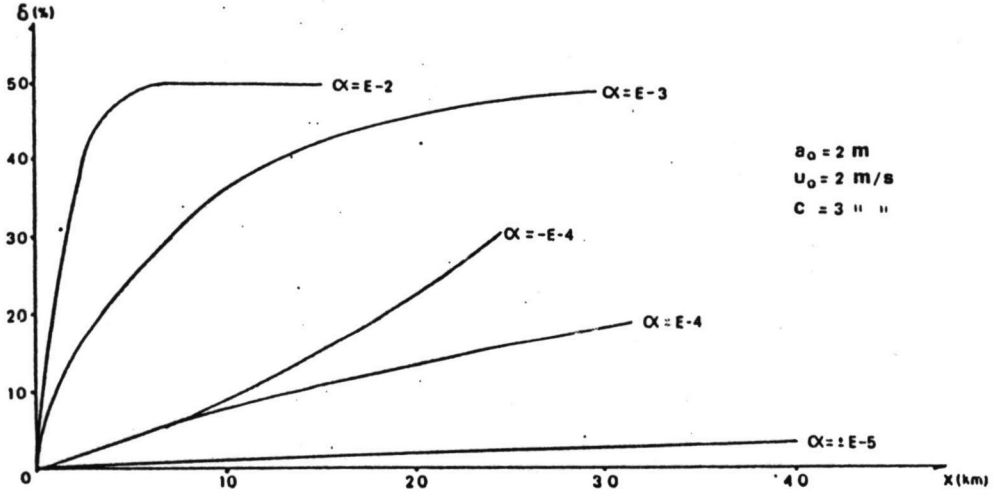

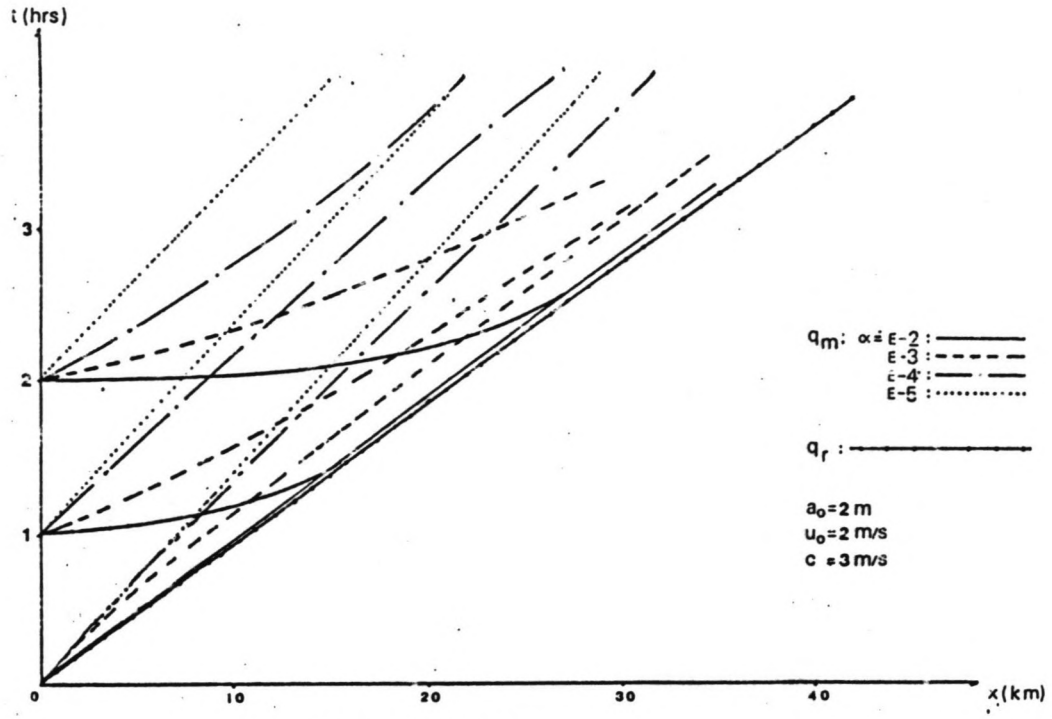

fig 9 x-t diagram

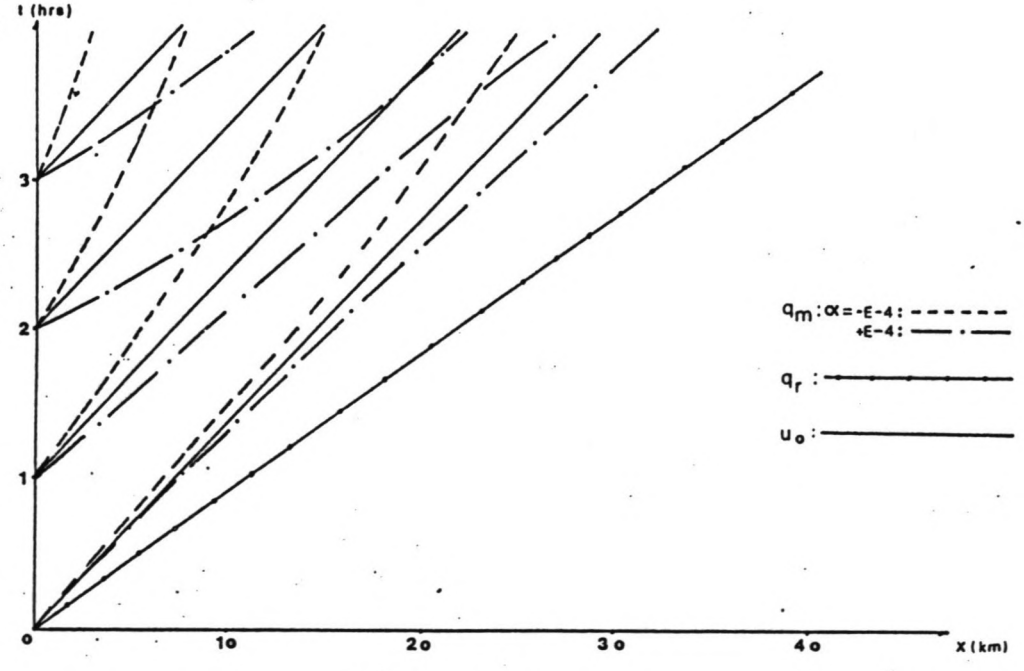

fig 10 x-t diagram

it follows that the measured discharge q_m passes point x at time t following from:

$$\frac{x}{c} \approx t + \frac{1}{\alpha}(u_o - c) - \left[t_o + \frac{1}{\alpha}(u_o - c)\right]\exp\left[-\frac{\alpha}{c}(t - t_o)\right]$$

whereas the actual discharge q_r passes point x at t following from:

$$t = t_o + x/c$$

This is illustrated in fig. 7.

Defining:

$$\varepsilon = \frac{q_r - q_m}{q_m}$$

and:

$$\delta = \max|\varepsilon|$$

it can be concluded, from computations made for several values of u_o, a_o and α, that:

(-) the maximum discrepancy δ between actual and measured discharge grows with distance (fig. 8). This is more pronounced for waves with $\alpha<0$ (a decreasing velocity) than for waves having $\alpha>0$.

(-) the discrepancies between actual and measured discharge are caused by differences in the waves' propagation velocities (fig. 9). The "mean" propagation velocity of a "complete" q_m-wave, that is, a wave consisting of both a part with $\alpha>0$ and a part having $\alpha<0$, would be about the base flow velocity u_o (fig. 10).

(-) maximum errors increase with increasing values of α (fig. 8).

The nature of these results give some back up for the numerical computations of Section 6.2.

6.4 Quantitative results

6.4.1. Theory

For a quantitative analysis of the relative error ε as a function of river and flow characteristics, a dimensional analysis can be used.

For a unit width, the governing equations are:

$$\frac{\delta u}{\delta t} + u\frac{\delta u}{\delta x} + g\frac{\delta a}{\delta x} - gi_b + g\frac{u^2}{C^2 a} = 0$$

$$\frac{\delta a}{\delta t} + u\frac{\delta a}{\delta x} + a\frac{\delta u}{\delta x} = 0$$

$$\frac{\delta \phi}{\delta t} + u\frac{\delta \phi}{\delta x} - \frac{1}{a}\frac{\delta}{\delta x}\left[(aK\frac{\delta \phi}{\delta x})\right] = 0$$

Choosing dimensionless variables as follows:

$A = a/a_o$
$U = u/u_o$
$\Phi = \phi/\phi_o$
$\Gamma = K/K_o$
$X = x/L_o$
$T = u_o t/L_o$

in which: a_o = base flow depth
u_o = base flow velocity
ϕ_o = base flow equilibrium concentration
$= M/Ba_o u_o$
K_o = base flow dispersion coefficient =
$= 0.0066 \cdot u_o^2 B^2/T_{yyo}$
L_o = base flow mixing length
$= 0.4 u_o B^2/T_{yyo}$
in which: $T_{yyo} = ka_o u_{*o}$
in which: k = coeff. of proportionality

Inserting these variables in the differential equations yields:

$$\frac{\delta U}{\delta T} + U\frac{\delta U}{\delta X} + g\frac{a_o}{u_o^2}\frac{\delta A}{\delta X} - g\frac{i_b L_o}{u_o^2} + g\frac{L_o U^2}{C^2 a_o A} = 0$$

$$\frac{\delta A}{\delta T} + U\frac{\delta A}{\delta X} + A\frac{\delta U}{\delta X} = 0$$

$$\frac{\delta \Phi}{\delta T} + U\frac{\delta \Phi}{\delta X} - \frac{K_o}{u_o L_o}\frac{1}{A}\frac{\delta}{\delta X}(A\Gamma\frac{\delta \Phi}{\delta X}) = 0$$

Using the Chézy relationship: $i_E = \frac{u_o^2}{C^2 a_o}$, it follows that:

$$\frac{\delta U}{\delta T} + U\frac{\delta U}{\delta X} + g\frac{a_o}{u_o^2}\frac{\delta A}{\delta X} - g\frac{L_o}{C^2 a_o}\left(1 - \frac{U^2}{A}\right) = 0$$

$$\frac{\delta A}{\delta T} + U\frac{\delta A}{\delta X} + A\frac{\delta U}{\delta X} = 0$$

$$\frac{\delta \Phi}{\delta T} + U\frac{\delta \Phi}{\delta X} - \frac{K_o}{u_o L_o}\frac{1}{A}\frac{\delta}{\delta X}\left(A\Gamma\frac{\delta \Phi}{\delta X}\right) = 0$$

in which the following dimensionless parameters can be recognized:

(-) $g\frac{a_o}{u_o^2} = Fr^{-2}$

(-) $g\frac{L_o}{C^2 a_o}$

(-) $\frac{K_o}{u_o L_o}$

The coefficient of proportionality for transverse dispersion is another dimensionless parameter:

(-) k

Through the boundary conditions, other dimensionless parameters are involved (fig. 11):

(-) a_{max}/a_o in which: a_{max} = maximum waterdepth

(-) $\frac{u_o}{L_o} T_g$

(-) Q, defining the flood wave's shape

The final dimensionless parameter determines the relative error between actual and measured discharge:

(-) $\varepsilon = \frac{AU - \Phi^{-1}}{\Phi^{-1}}$

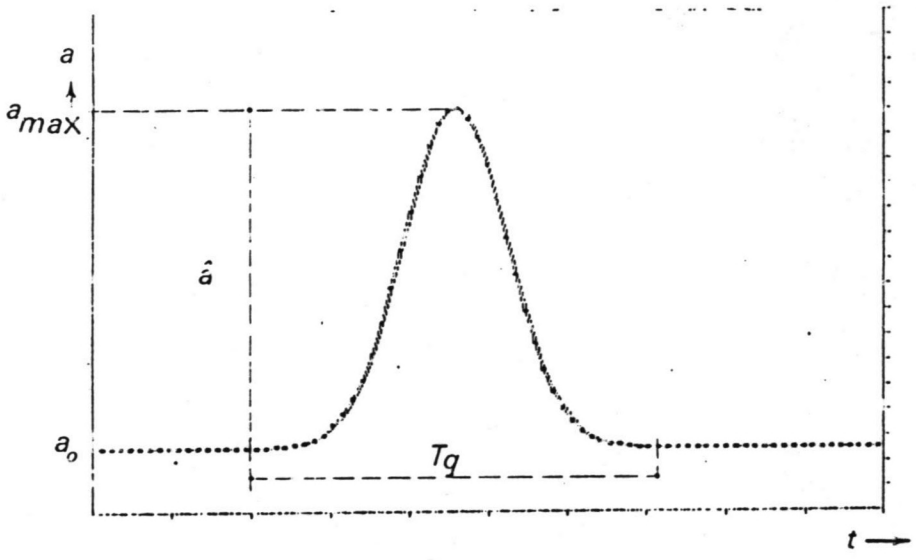

Fig 11 Gaussian Flood wave

6.4.2 Practical approach

With some reasoning and limitations, the number of dimensionless parameters involved, can be reduced.
Firstly, it has been shown (Chapter III) that the dispersion model's application is essentially restricted to flood waves that can be described by the diffusion analogy ($T_g >> T_c$). This has the consequence that two parameters Fr^{-2} and gL_o/C^2a_o can be replaced by one parameter:

$$(-)\ \frac{i_b L_c}{a_o}$$

Secondly, only flood waves of Gaussian distribution are considered, so the parameter Q is not taken into account.
Thirdly, the distance from the point of injection L_o is taken minimal. From eq. 8 and 10, it then follows that:

$$K_o = 0.0165 \cdot u_o L_o$$

which yields for the parameter $K_o/u_o L_o$ a fixed value:

$$(-)\ \frac{K_o}{u_o L_o} = 0.0165$$

Finally, only maximum errors are considered, so the error fluctuation during flood wave passage is not taken into account. This yields instead of the parameter ε:

$$(-)\ \delta = \max|\varepsilon|$$

Resuming, this parameter δ is now described by:

$$(-)\ k$$

$$(-)\ \frac{i_b L_o}{a_o}$$

$$(-)\ \frac{a_{max}}{a_o}$$

$$(-)\ \frac{u_o}{L_o} T_g$$

This latter parameter can be written as (eq. 9 and 10):

$$\frac{u_o}{L_o} T_g = 2.5\ T_g/T_c$$

So this leaves the maximum error δ described by:

(-) k

(-) $\frac{i_b L_o}{a_o}$

(-) $\frac{a_{max}}{a_o}$

(-) T_g/T_c

All computations made have shown no significant trend in the influence of the parameter $i_b L_o/a_o$ on the error magnitude. Examples are given in fig. 12.
For larger values of T_g/T_c, this may be explained by realising that damping of the flood wave over the mixing length is of minor importance. Moreover, from the qualitative analysis in Section 6.2, it followed that, for all values of T_g/T_c, wave damping contribution to the error magnitude is of minor importance compared to the influence of the difference in propagation velocities.
Omitting distinction to the parameter $i_b L_o/a_o$, which, in fact, means a kinematic wave evaluation of the dynamic wave computation, yields the following graphs (fig. 13 and 14), in which the influence of the parameter k is shown.
Since the value of the parameter $K_o/u_o L_o$ is fixed at 0.0165, the parameter k influences, through T_c, only the value of T_g/T_c. It is to be expected that the smaller values of k will yield, through larger mixing lengths, the larger errors. From the nature of the graphs, it is clear that for the larger values of T_g/T_c, however, there should be no significant difference in error magnitude for different values of k.
Fig. 13 seems to illustrate this for values of k=0.25 and k=0.60. Computations made with values of k=0.95, however, obscure these results in showing no significant smaller errors compared to the computations with smaller values of k (fig. 14). Values of k will, in the field, be hard to determine accurately, and their influence being not very pronounced, it has been decided, in view of a practical approach, to omit distinction to the transverse diffusivity coefficient as well.
This leaves in fig. 15 the maximum errors defined by a_{max}/a_o and T_g/T_c.
Drawing regression lines through and near points of equal a_{max}/a_o finally gives fig. 16.
For known values of the parameter a_{max}/a_o and T_g/T_c and for values of the other parameters within their indicated ranges, the maximum relative error can be estimated from fig. 16.
In the field, the parameter a_{max}/a_o can be measured by (continuous) stage recording.
Estimating the parameter T_g/T_c (or $(u_o/L_o)\cdot T_g$), however, is more difficult. Even if the flood wave period is known (from e.g. the stage recording), the value of T_c (or u_o/L_o) will be hard to determine, since the base flow velocity u_o is not known and the

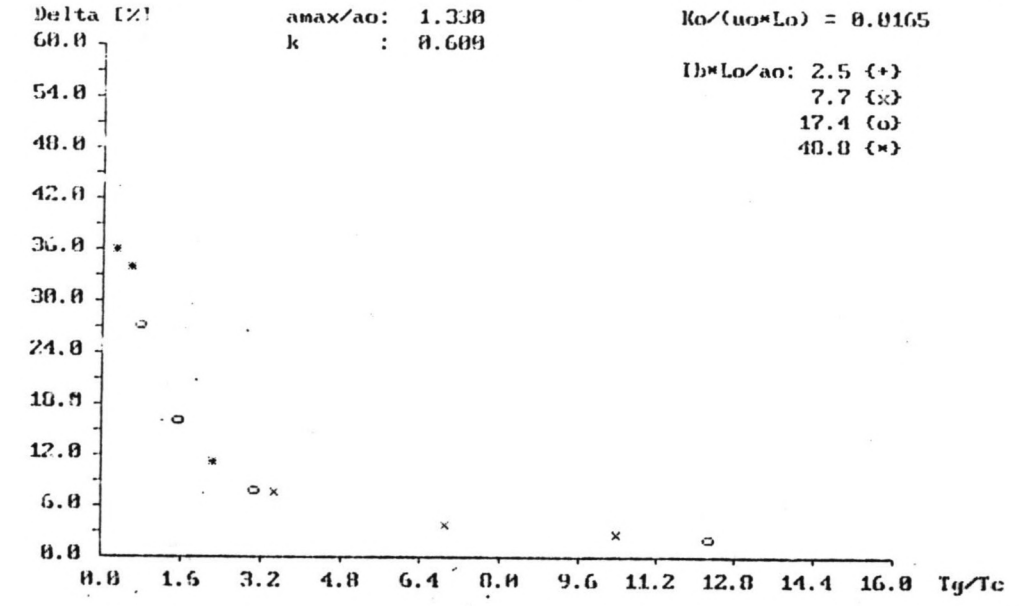

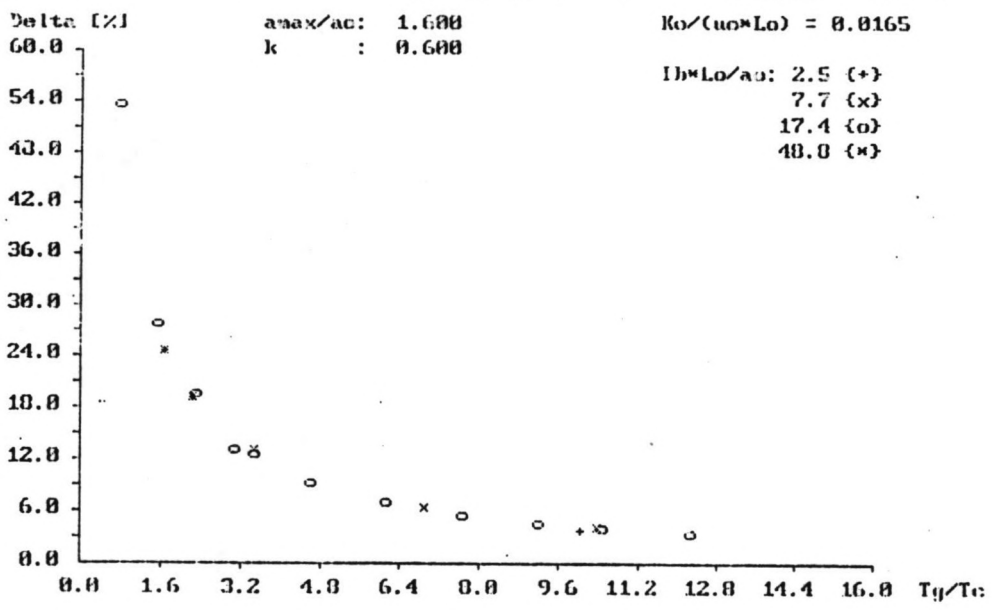

Fig 12 Influence of $Ib*Lo/a_o$

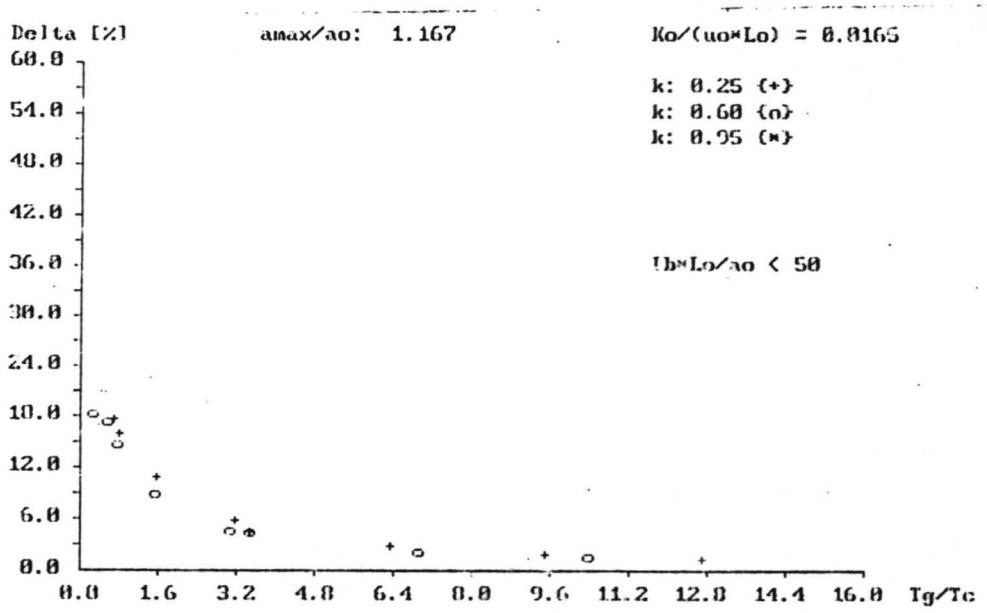

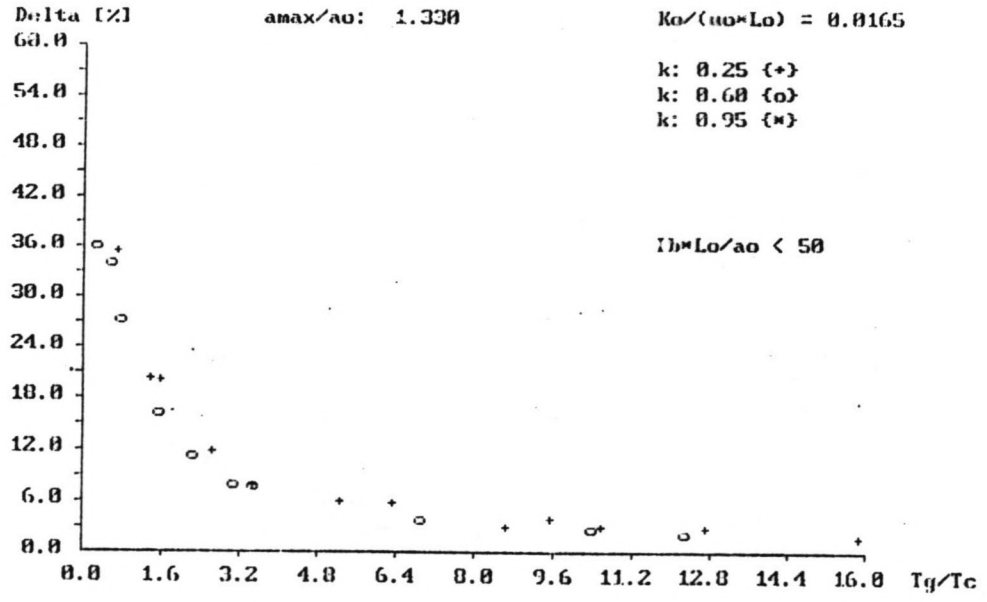

Fig 13 Influence of k

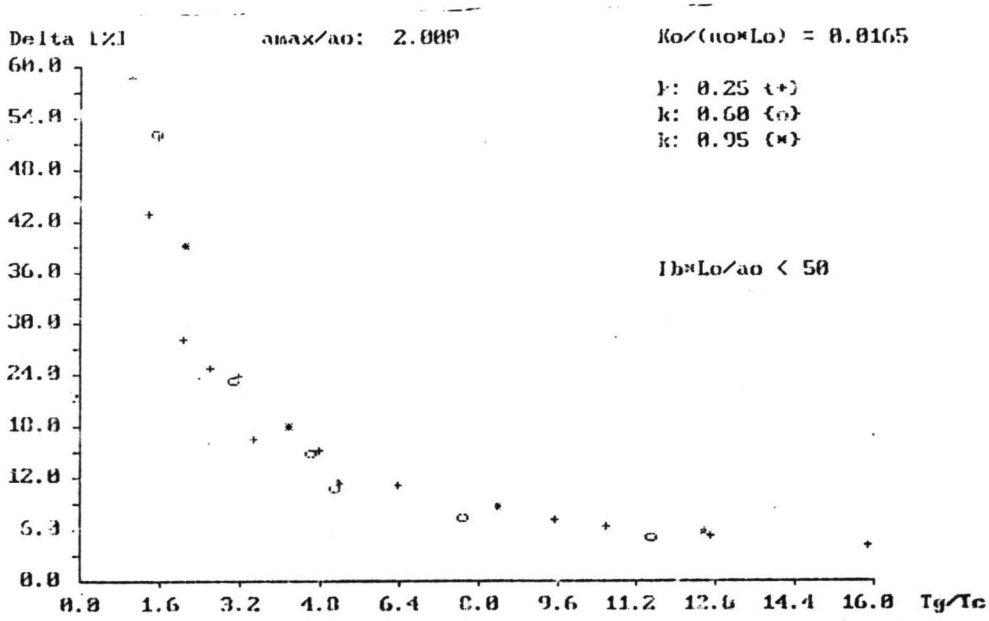

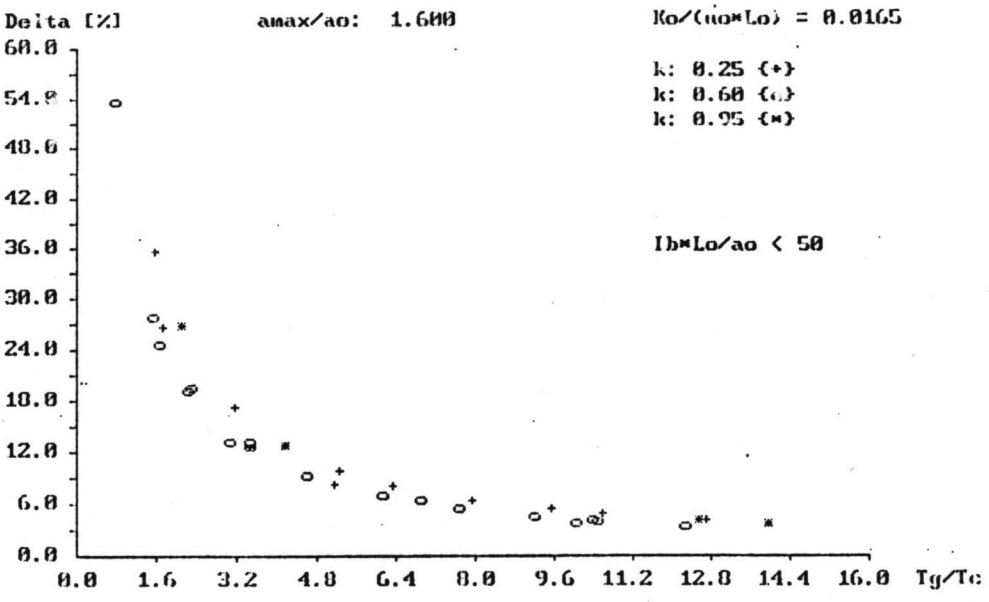

Fig 14 Influence of k

Fig 15 δ

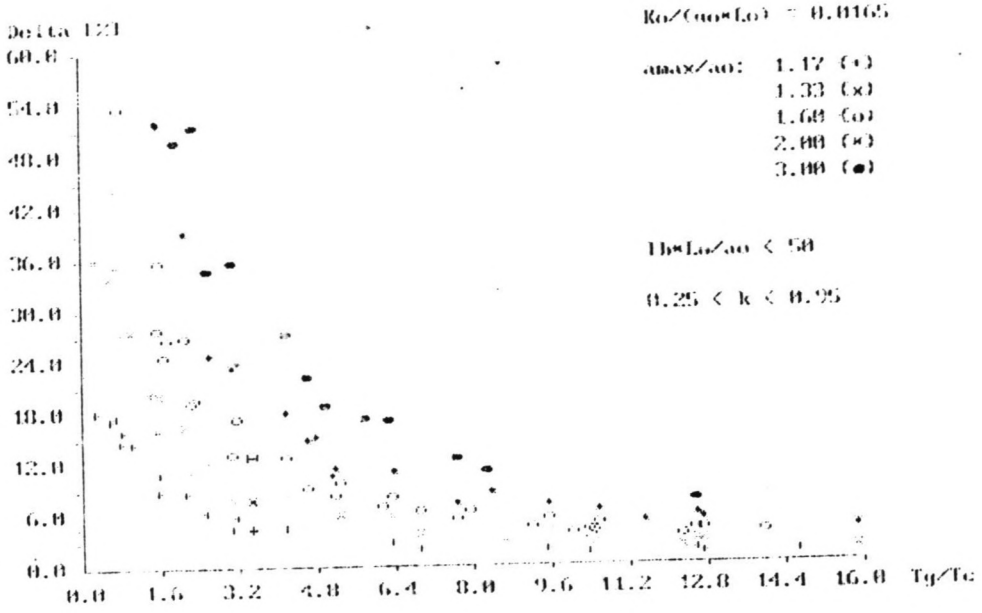

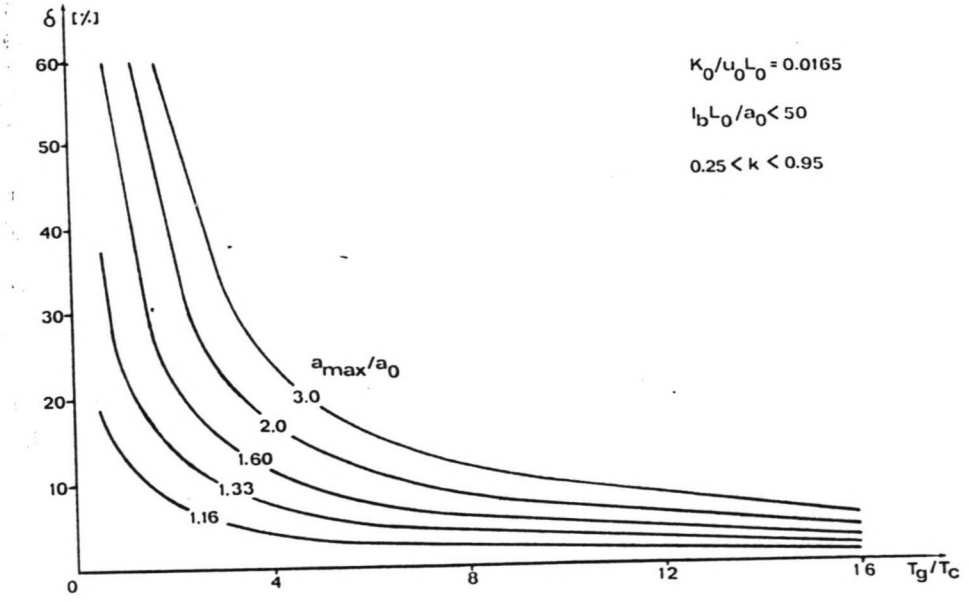

Fig 16 δ– curves

actual mixing length in the field L_r will, no doubt, differ from the semi-theoretical value L_o.
An approximate procedure can be, to estimate a velocity u_m from the measured discharge Q_m:

$$u_m \approx \frac{Q_m}{B \cdot a_m}$$

in which: a_m = measured depth
u_m = estimated velocity

and computing:

$$T_g/T_c \Big|_m \approx 0.4 \cdot \frac{u_m}{L_r} \cdot T_g$$

in which: L_r = actual mixing length
$T_g/T_c \Big|_m$ = estimated value of T_g/T_c

as an indicator for T_g/T_c.
From fig. 16 it then follows whether or not a discrepancy between the actual and estimated value of T_g/T_c has much influence on the maximum error determination.

6.4.3 Evaluation

It can be concluded from fig. 16 that maximum errors can easily be an order of magnitude larger than the 1% relative error during steady flow conditions (Chapter II). The actual error at the time of measurement t_m, of course, may well be much smaller (fig. 1). Nevertheless, an attempt to improve the measurement's result is welcome. This can be done by an iterative procedure.
In a first approximation, such a procedure could be to estimate the time lag from:

$$t_d \approx \frac{L_r}{u_m} - \frac{L_r}{1.5 \cdot u_m} = \frac{L_r}{3 \cdot u_m}$$

in which: t_d = estimated time lag

It is hereby assumed that the measured velocity u_m is a good approximation of the Q_m-wave's propagation velocity and that the Q_r-wave travels 1.5 times as fast (Section 6.2).
Using the Chezy relationship, it follows for constant Chezy-coefficient:

$$Q = f(a^{3/2})$$

and so an iterative procedure could be:

$$Q_r(t_m) \approx Q_m^*(t_m) = Q_m(t_m)\left[\frac{a_m(t_m)}{a_m(t_m-t_d)}\right]^{3/2}$$

in which: t_m = time of measurement

An example of the behaviour of the relative error in time after this correction procedure is typically shown in fig. 17.
From estimating the time lag, a second approximation can be given:

$$Q_r(t_m-t_d) \approx Q_m(t_m)$$

An example of the behaviour of the relative error after this correction has already been shown in fig. 6.
Both procedures are illustrated in fig. 18.
Compared to the original errors their improvements are obvious, although in the field their effects will, no doubt, be less pronounced. Apart from nature's variability causing differences between the actual mean flow velocity, the actual propagation velocity and their indicated estimations u_m and $1.5 \cdot u_m$, the measurements in the field will also be obscured by measurement errors and 'noise' in e.g. the stage-recording.
Both procedures will be even more sophisticated using the Jones formula instead of the Chezy stage-discharge relationship and by estimating the time lag from that stage-discharge relationship (Chapter V):

$$t_d^* \approx \frac{L_r}{u_m} - \frac{L_r}{c_m}$$

in which: $c_m = \frac{1}{B}\cdot\frac{dQ_m}{da_m}$ = estimated Q_r-wave propagation velocity

and so for constant roughness this yields the following corrections:

$$Q_r(t_m) \approx Q_m^{**}(t_m) = Q_m(t_m)\left[\frac{\left[a_m^3\left[i_b + \frac{1}{c_m}\cdot\frac{\delta a_m}{\delta t}\right]\right]_{t_m}}{\left[a_m^3\left[i_b + \frac{1}{c_m}\cdot\frac{\delta a_m}{\delta t}\right]\right]_{t_m-t_d^*}}\right]^{1/2}$$

and

$$Q_r(t_m-t_d^*) \approx Q_m(t_m)$$

The improvements of these correction procedures over the previous ones have not been investigated. It is clear, however, that these last iterations require more measurements.

fig 17 correction procedure: Qm*: thin line

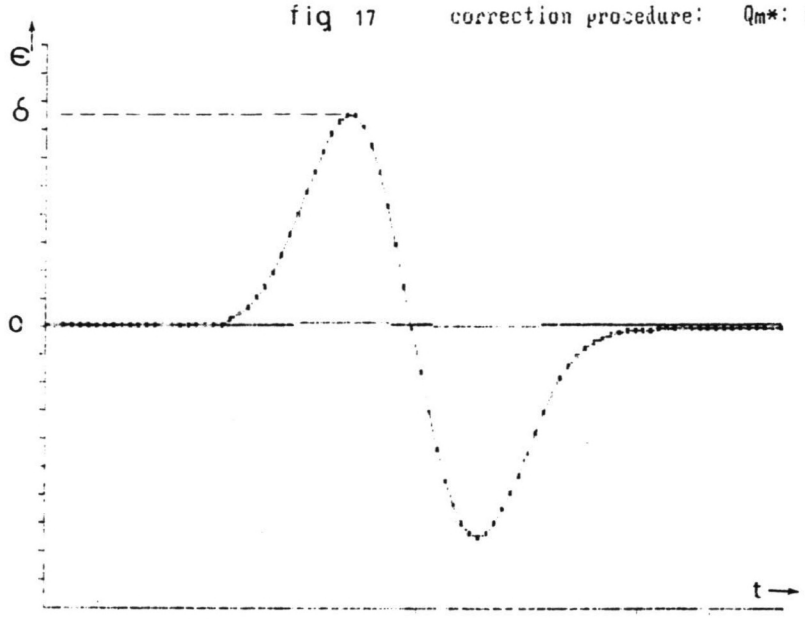

Fig 18 Iterations

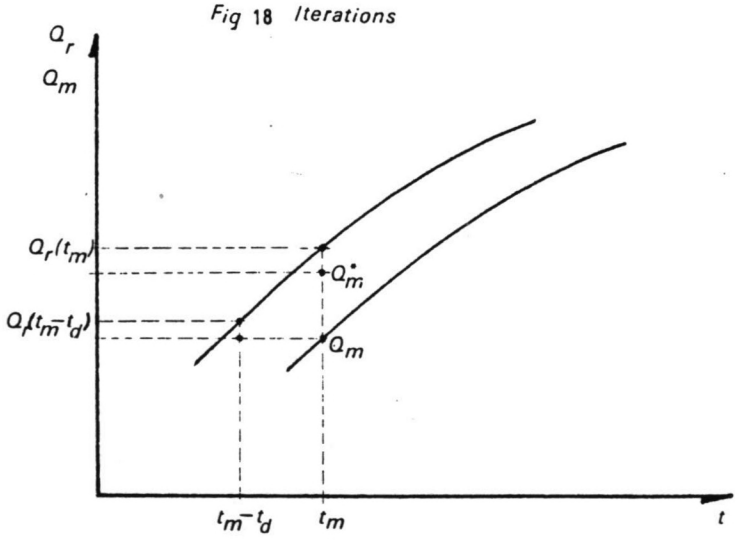

As an additional feature, the estimated time lag, together with an estimation of the flood wave period (from e.g. the stage recordings), provide a means of evaluating the order of magnitude of the actual relative error ε compared to its maximum value δ (Section 6.2). For small values of the ratio t_d/T_g the maximum errors (positive and negative (fig. 1)) occur near or at the fast rising and falling parts of the hydrograph. For larger values of t_d/T_g the maximum errors will occur later in the flood wave period.
This is illustrated in fig. 19.

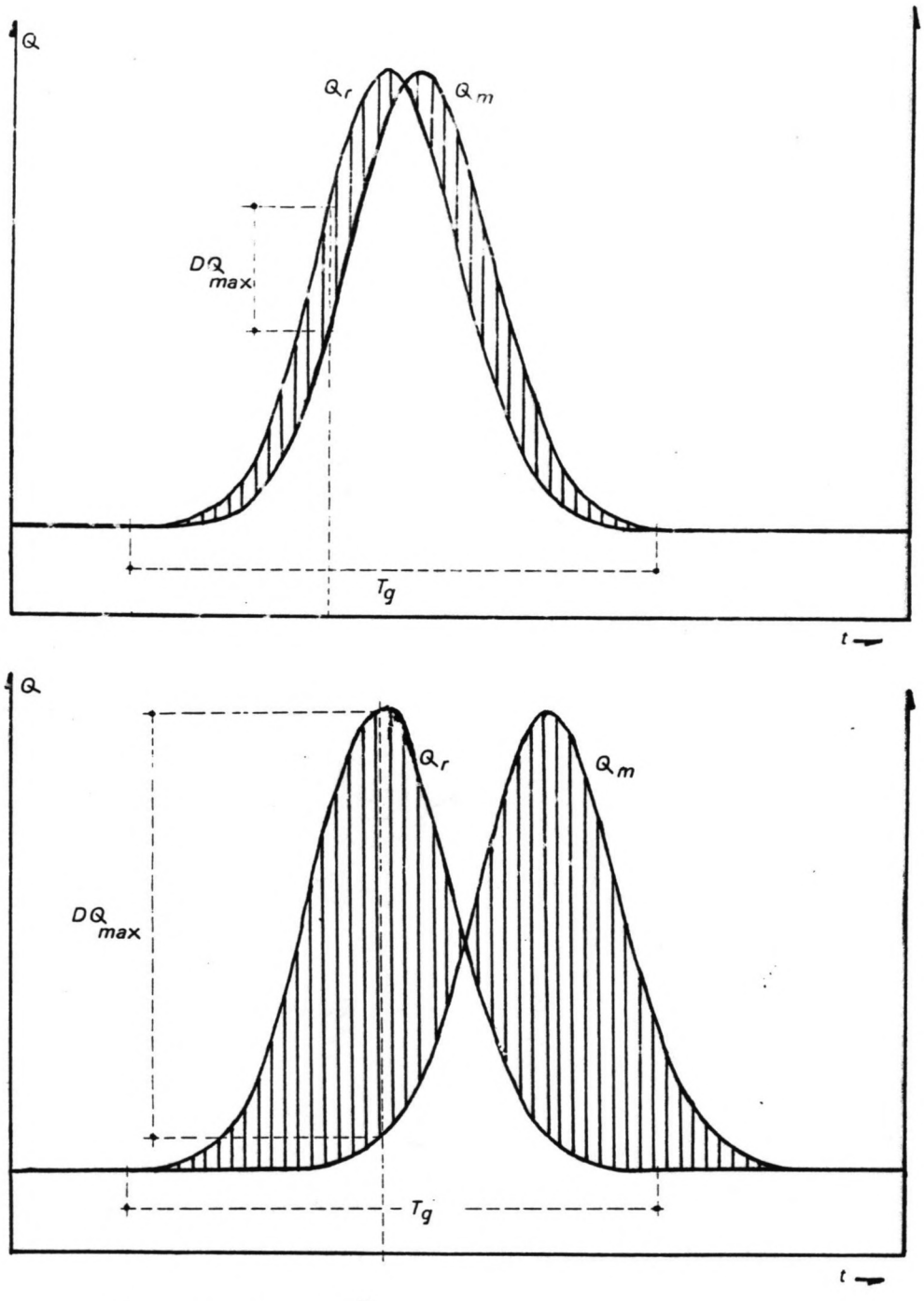

FIG 19 TIME OF **6.**

CHAPTER VII CONCLUSIONS AND RECOMMENDATIONS

In view of a practical approach to constant rate dilution discharge measurements during flood waves, the errors relative to measurements during steady flow are evaluated, by determining the discharge from the concentration distribution (or 'chemograph'), using an extended steady state relationship:

$$Q_m(L,t) = \frac{M}{\phi(L,t)}$$

in which: Q_m = measured discharge
M = constant tracer amount released per unit time
ϕ = concentration
L = mixing length
t = time

In the computational model, such a discharge measurement is simulated. The discrepancy between the "measured discharge" Q_m and the "actual discharge" Q_r defines the relative error:

$$\varepsilon(L,t) = \frac{Q_r(L,t)-Q_m(L,t)}{Q_m(L,t)}$$

in which: Q_r = actual discharge
ε = relative error

Computations made for Gaussian shaped flood waves propagating down a channel of rectangular, uniform cross-section, yield the maximum relative error δ:

$$\delta = \max|\varepsilon|$$

as a function of dimensionless parameters in fig. 1.

Within the indicated ranges of the relevant parameters the magnitude of the maximum relative error δ is significantly influenced only by two parameters:

a_{max}/a_0 : a measure for the flood wave's amplitude

T_g/T_c : a measure for the flood wave's length compared to the mixing length

The main error source is a phase shift between the actual and the measured discharge. This phase shift is caused by the difference in propagation velocity of the tracer cloud and the flood wave.

Since the maximum errors δ can easily be larger by an order of magnitude than the 1% relative error achievable during steady flow conditions, correction procedures are recommended. Based on estimating the time lag between both waves from the known mixing length and the measured discharge. It is thereby assumed that (continuous) stage recording is part of the measurement campaign. An additional feature of the time lag estimation is that one discharge measurement yields approximations of the actual discharge at two different time levels.
Moreover, from comparing the estimated time lag to the flood wave period, together with the stage recordings the order of magnitude of the actual relative error ε compared to its maximum value δ can be evaluated.

Since nature rarely directs exactly Gaussian shaped flood waves down rivers of rectangular and uniform cross-section, these results have but an indicative value.
Laboratory and field experiments and more computational work to take account of nature's variability are therefore recommended as topics for further study.

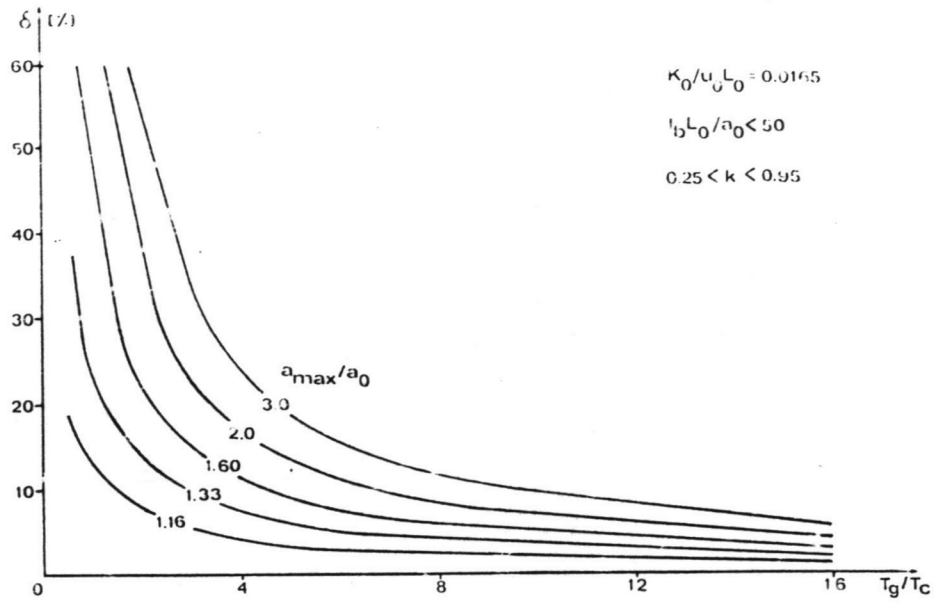

Fig 1 δ– curves

LIST OF IMPORTANT SYMBOLS

symbol		dimension
a	depth	$[L]$
a_0	base flow depth	$[L]$
a_m	measured depth	$[L]$
a_{max}	maximum depth	$[L]$
A	cross-section	$[L^2]$
A_0	base flow cross-section	$[L^2]$
B	width	$[L]$
c	propagation velocity	$[LT^{-1}]$
c_m	estimated propagation velocity	$[LT^{-1}]$
c_r	relative celerity per wave period	$[LT^{-1}]$
C	Chezy coefficient	$[L^{1/2}T^{-1}]$
d_n	damping factor per wave period	$[-]$
d_r	damping factor per relaxation time	$[-]$
D	molecular diffusion coefficient	$[L^2T^{-1}]$
D_c	characteristic diffusivity	$[L^2T^{-1}]$
D_t	time step	$[T]$
D_x	mesh width	$[L]$
D_φ	flow weighted degree of mixing	$[-]$
E	dimensionless parameter	$[-]$
F_r	Froude number	$[-]$
F_s	forces in s-direction	$[MLT^{-2}]$
F_x	mass flux in x-direction	$[ML^{-2}T^{-1}]$
g	gravity acceleration	$[LT^{-2}]$
h	water level	$[L]$
i_b	bottom slope	$[-]$
k	coefficient of proportionality	$[-]$
k_φ	wave number	$[L^{-1}]$
K	dispersion coefficient	$[L^2T^{-1}]$
K_{eff}	effective dispersion coefficient	$[L^2T^{-1}]$
K_{num}	numerical dispersion coefficient	$[L^2T^{-1}]$
K_0	base flow dispersion coefficient	$[L^2T^{-1}]$
K_{osc}	dispersion coefficient in oscillating flow	$[L^2T^{-1}]$
L	mixing length	$[L]$
L_c	characteristic length	$[L]$
L_φ	flood wave length	$[L]$
L_i	length of initial zone	$[L]$
L_r	actual mixing length	$[L]$
$L_{0,95}$	cross-sectional mixing length for 95% mixing	$[L]$
m	released tracer amount	$[M]$
M	const. tracer amount released per unit time	$[MT^{-1}]$
n	number of time steps	$[-]$
P	cell-Peclet number	$[-]$

q_m	measured discharge per unit width	$[L^2T^{-1}]$
q_r	actual discharge per unit width	$[L^2T^{-1}]$
Q	discharge	$[L^3T^{-1}]$
Q_m	measured discharge	$[L^3T^{-1}]$
Q_o	base flow discharge	$[L^3T^{-1}]$
Q_r	actual discharge	$[L^3T^{-1}]$
r	friction factor	$[T^{-1}]$
R	hydraulic radius	$[L]$
s	bottom slope directed coordinate	$[-]$
t	time	$[T]$
t_d	estimated time lag	$[T]$
t_e	relaxation time	$[T]$
t_m	time of measurement	$[T]$
T_c	characteristic time	$[T]$
T_d	dimensionless time	$[-]$
T_g	flood wave period	$[T]$
T_i	initial time	$[T]$
T_{yy}	transverse diffusivity	$[L^2T^{-1}]$
T_{yyo}	base flow transverse diffusivity	$[L^2T^{-1}]$
u	flow velocity in x-direction	$[LT^{-1}]$
u_m	estimated velocity	$[LT^{-1}]$
u_o	base flow velocity	$[LT^{-1}]$
u_*	bottom shear flow velocity	$[LT^{-1}]$
u_{*o}	base flow bottom shear velocity	$[LT^{-1}]$
v	flow velocity in y-direction	$[LT^{-1}]$
w	flow velocity in z-direction	$[LT^{-1}]$
x	longitudinal coordinate	$[-]$
X_d	dimensionless distance	$[-]$
y	transverse coordinate	$[-]$
z	vertical coordinate	$[-]$
α	coefficient	$[LT^{-2}]$
β	coefficient	$[LT^{-1}]$
δ	maximum relative error	$[-]$
ε	relative error	$[-]$
θ	weighing factor	$[-]$
ϱ	flood wave shape factor	$[L]$
μ	density	$[ML^{-3}]$
τ_b	bottom friction	$[ML^{-1}T^{-2}]$
ϕ	concentration	$[ML^{-3}]$
ϕ_i	initial concentration	$[ML^{-3}]$
ϕ_o	base flow equilibrium concentration	$[ML^{-3}]$

BIBLIOGRAPHY

Abramowitz M. and Stegun I.A. (1965)
'Handbook of mathematical functions'
Dover Public. Inc.,New York

Allersma E. (1973)
'Hydraulics of open water management'
in: Proc. Techn. Meeting 26
'Hydraulic research for water management'
Committee for hydrological research TNO, The Hague

Berkhoff J.C.W. (1973)
'Transport of pollutants or heat in a system of channels'
in: Proc. Techn. Meeting 26
'Hydraulic research for water management'
Committee for hydrological research TNO, The Hague

Booij R. (1986)
'Turbulentie in de waterloopkunde'
Lecture notes b82
Dep. of Civil Engineering, Techn. Univ. Delft

Chatwin P.C. (1970)
'The approach to normality of the concentration distribution of a solute in a solvent flowing along a straight pipe'
J. Fluid Mech. 43

Chatwin P.C. (1975)
'On the longitudinal dispersion of passive containment in oscillatory flows in tubes'
J. Fluid Mech. 71

Craenenbroeck W. van and Marivoet J. (1987)
'A comparison of simple methods for estimating the mass flow of fluoride discharged into rivers'
Wat. Sci. Techn. Vol. 19, Rio

Crank J. (1975)
'The mathematics of diffusion'
Clarendon Press, Oxford (2nd ed.)

Fischer H.B. (1967)
'The mechanisms of dispersion in natural streams'
Proc. ASCE 93 Hy6

Fischer H.B. et al. (1979)
'Mixing in inland and coastal waters'
Academic Press, New York

Glover B. and Johnson P. (1974)
'Variations in the natural chemical concentration of river water during flood flows'
J. Hydrol. 22

Goslinga J. and Verboom G.K. (1979)
'Mathematical techniques to determine longitudinal dispersion coefficients and concentration distributions. A review of the Taylor and the Aris method'
Delft Hydr. Lab. Report 1092

Grijsen J.G. and Vreugdenhil C.B. (1976)
'Numerical representation of flood waves in rivers'
Delft Hydr. Lab. Publ. 165

Hemingway E. (1977), first published 1933
'The torrents of spring'
Granada Publ. Ltd, London

Holley E.R.,Harleman D.R.F.,Fischer H.B. (1970)
'Dispersion in homogeneous estuary flow'
Proc. ASCE 96 Hy8

Hubbard E.F.,Kilpatrick F.A.,Martens L.A.,Wilson J.F.Jr. (1982)
'Measurement of time of travel and dispersion in streams by dye tracing'
U.S. Geol. Survey, Techn. Wat. Res. Inv., Book 3, Chapter A9
U.S. Governm. Printing Off., Washington

ISO (1986)
'Liquid flow measurements in open channels. Dilution methods (TC 113/SC4). Mixing length in open channels'
Draft techn. report

Jansen P. Ph. et al. (1979)
'Principles of river engineering'
Pitman, London

Kilpatrick F.A. and Cobb E.D. (1985)
'Measurement of discharge using tracers'
U.S. Geol. Survey, Techn. Wat. Res. Inv., Book 3, Chapt. A16
U.S. Governm. Printing Off., Washington

Mazijk A. van (1984)
'Dispersie in rivieren'
Report 16-83
Dep. of Civil Engineering, Techn. Univ. Delft

Nes Th.J. van de, Hendriks M.H. (1971)
'Analysis of a linear distributed model of surface run off'
Lab. of Hydraulics and Catchment Hydrology
Agric. Univ., Wageningen

Sayre W.W. (1975)
'Dispersion of mass in open channel flow'
Hydrology paper 75
Colorado State Univ., Fort Collins, Colorado

Taylor G.I (1953)
'Dispersion of soluble matter in solvent flowing slowly through a tube'
Proc. R. Society London Ser. A 219

Taylor G.I (1953)
'The dispersion of matter in turbulent flow through a pipe'
Proc. R. Society London Ser. A 223

Urbanus J.F.X. and Vreeburg J.H.G. (1987)
'Calamiteitenmodel Noordelijk Deltabekken'
M.Sc. thesis (unpublished)
Dep. of Civil Engineering, Techn. Univ. Delft

Verspuy C., Vries M. de (1981)
'Lange golven'
Lecture notes b73
Dep. of Civil Engineering, Techn. Univ. Delft

Vreugdenhil C.B. (1973)
'Computational methods for channel flow'
in: Proc. Techn. Meeting 26
'Hydraulic research for water management'
Committee for hydrological research TNO, The Hague

Vreugdenhil C.B. (1982)
'Numerical effects in models for river morphology'
In: M.B. Abbott and J.A. Cunge (Eds.)
'Engineering applications of computational hydraulics'
Vol. I, Pitman, London

Vreugdenhil C.B. (1985)
'Numerieke berekeningen in waterbouwkunde en hydrologie'
Lecture notes b84N
Dep. of Civil Engineering, Techn. Univ. Delft

Vries M. de (1984)[1]
'Inleiding vloeistofmechanica'
Lecture notes b70
Dep. of Civil Engineering, Techn. Univ. Delft

Vries M. de (1984)[2]
'Vloeistofmechanica'
Lecture notes b71N
Dep. of Civil Engineering, Techn. Univ. Delft

Vries M. de (1986)[1]
'Metingen waterbouwkunde en hydrologie'
Lecture notes f29
Dep. of Civil Engineering, Techn. Univ. Delft

Vries M. de (1986)[2]
'Rivierwaterbouwkunde b.o.'
Lecture notes f13B
Dep. of Civil Engineering, Techn. Univ. Delft

Walling D.E. and Webb B.W. (1980)
'The spatial behaviour in the interpretation of stream solute behaviour'
J. Hydrol. 47

Whitham G.B. (1974)
'Linear and non linear waves'
Wiley, New York

Wilson J.F.Jr.,Cobb E.D., Kilpatrick F.A. (1984)
'Fluorometric procedures for dye tracing'
U.S. Geol. Survey, Techn. Wat. Res. Inv., Book 3, Chapt. A12
U.S. Governm. Printing Off., Washington

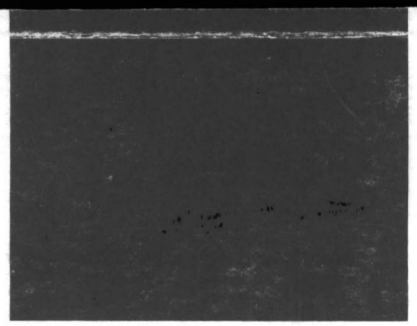

882505